



HAL
open science

Deciphering the recombinant thermostable phosphatidylcholine-specific phospholipase C activity from *Bacillus thuringiensis*: Biochemical and interfacial properties

Ahlem Eddehech, Nabil Smichi, Sebastien Violot, Emmanuel Bettler, Leyre Brizuela, Alexandre Noiriél, Abdelkarim Abousalham, Zied Zarai

► To cite this version:

Ahlem Eddehech, Nabil Smichi, Sebastien Violot, Emmanuel Bettler, Leyre Brizuela, et al.. Deciphering the recombinant thermostable phosphatidylcholine-specific phospholipase C activity from *Bacillus thuringiensis*: Biochemical and interfacial properties. *Colloids and Surfaces A: Physicochemical and Engineering Aspects*, 2021, 630, pp.127629. 10.1016/j.colsurfa.2021.127629 . hal-04669847

HAL Id: hal-04669847

<https://hal.science/hal-04669847v1>

Submitted on 13 Nov 2024

HAL is a multi-disciplinary open access archive for the deposit and dissemination of scientific research documents, whether they are published or not. The documents may come from teaching and research institutions in France or abroad, or from public or private research centers.

L'archive ouverte pluridisciplinaire **HAL**, est destinée au dépôt et à la diffusion de documents scientifiques de niveau recherche, publiés ou non, émanant des établissements d'enseignement et de recherche français ou étrangers, des laboratoires publics ou privés.



Distributed under a Creative Commons Attribution - NonCommercial 4.0 International License

Deciphering the recombinant thermostable phosphatidylcholine-specific phospholipase C activity from *Bacillus thuringiensis*: biochemical and interfacial properties

Ahlem EDDEHECH^{a,f}, Nabil SMICHI^b, Sebastien VIOLOT^c, Emmanuel BETTLER^d, Leyre BRIZUELA^e, Alexandre NOIRIEL^f, Abdelkarim ABOUSALHAM^{f,*}, Zied ZARAI^{a,g,*}

^a University of Sfax, ENIS, Laboratory of Biochemistry and Enzymatic Engineering of Lipases, Sfax, Tunisia.

^b Mayo Clinic Arizona, 13400 Shea Boulevard, Scottsdale, AZ, 85259, USA.

^c Molecular Microbiology and Structural Biochemistry, UMR 5086, CNRS Université de Lyon, 7 passage du Vercors, 69367 Lyon, France

^d Tissue Biology and Therapeutic Engineering Laboratory (LBTI), UMR 5305, CNRS Université de Lyon, 7 passage du Vercors, 69367 Lyon, France.

^e Univ Lyon, Université Lyon 1, Institut de Chimie et de Biochimie Moléculaires et Supramoléculaires (ICBMS), UMR 5246 CNRS, Métabolisme, Enzymes et Mécanismes Moléculaires (MEM2), Bât Raulin, 43 Bd du 11 Novembre 1918, F-69622 Villeurbanne Cedex, France.

^f Univ Lyon, Université Lyon 1, Institut de Chimie et de Biochimie Moléculaires et Supramoléculaires (ICBMS), UMR 5246 CNRS, Génie Enzymatique, Membranes Biomimétiques et Assemblages Supramoléculaires (GEMBAS), Bât Raulin, 43 Bd du 11 Novembre 1918, F-69622 Villeurbanne Cedex, France.

^g High Institute of Biotechnology of Sfax, food technology department, Sfax, Tunisia.

(*) Corresponding authors:

Abdelkarim Abousalham, E-mail: abdelkarim.abousalham@univ-lyon1.fr

Zied Zarai, E-mail: zarai.zied@hotmail.fr

Abstract

1 A novel alkaline thermostable phosphatidylcholine-specific phospholipase C (PC-PLC_{Bt}) was
2 expressed in *E. coli* system. Recombinant PC-PLC_{Bt} (rPC-PLC_{Bt}) activity and thermostability
3 were shown to be significantly dependent on the Zn²⁺. The maximum rPC-PLC_{Bt} catalytic
4 activity was found to be 1372 U.mg⁻¹ in the presence of 0.1 mM Zn²⁺ and at 60 °C using an
5 Egg PC as substrate. The interfacial kinetic data show that nPC-PLC_{Bt} and rPC-PLC_{Bt} display
6 similar substrate specificity on various phospholipid monolayers. The maximal rPC-PLC_{Bt}
7 activities were recorded, at decreasing order, on 1,2-dilauroyl-*sn*-glycero-3-phosphocholine
8 (DLPC), 1,2-dilauroyl-*sn*-glycero-3-phosphoethanolamine (DLPE), 1,2-diacyl-*sn*-
9 phosphoglycerol (PG), and 1,2-diacyl-*sn*-phosphoserine (PS) monolayers at interfacial surface
10 pressures of 15, 25, 20, and 25 mN.m⁻¹, respectively. Such important penetrating power could
11 be exploited for pharmacological purposes. The highest activities were recorded on the DLPC
12 monolayer and shown to be 121.61 and 40.13 mmol.cm⁻².min⁻¹.M⁻¹ for native and
13 recombinant PC-PLC_{Bt}, respectively. Interestingly, compared to all known *Bacillus* PLCs,
14 both PC-PLC_{Bt} forms showed an exclusive capacity to hydrolyze the PG film with a more
15 pronounced rate of hydrolysis for the native form with a specific activity of 58.29 mmol.cm⁻².min⁻¹.M⁻¹.
16 Therefore, the high enzyme level production of about 14 mg.L⁻¹, the
17 thermostability as well as the broad phospholipid specificity of PC-PLC_{Bt} represents great
18 potential in the crude oil refining industry.

19 **Keywords:** *B. thuringiensis* IL14; PC-PLC; thermostability; substrate specificity; interfacial
20 properties; cytotoxic properties.

21
22
23
24
25
26

27 **1.Introduction:**

28 Phosphatidylcholine-phospholipase C (PC-PLC) is a lipolytic enzyme that preferentially
29 hydrolyzes the PC, as a major substrate, as well as other kinds of phospholipids, into 1,2-
30 diacylglycerol (1,2-DAG) and the correspondent phosphate monoesters [1]. Bacterial PC-PLC
31 is the most promising enzyme for application in the enzymatic degumming of plant oils,
32 considering its high activity, easy production, wide substrate spectrum, and approved safety
33 [2, 3]. It offers the opportunity of oil enrichment with released DAG and contributes to the
34 final oil yield [4]. Moreover, the microbial PLC appeared as a potentially useful model for
35 mammals PC-PLC to study cellular signaling, lipid metabolism, blood coagulation, and
36 eukaryotic cell membranes [5]. *Bacillus cereus* PLC (PLC_{Bc}) is the most studied among the
37 bacterial PC-PLC. It is an extracellular monomeric zinc-dependent enzyme of 28.5 kDa
38 synthesized as a 283 residues pre-proenzyme from which the 24-residue long signal peptide
39 and the 14-residue long pro-peptide are cleaved to give a fully active enzyme [3].
40 Crystallographic [6, 7] and chemical modification [8] studies of the PC-PLC_{Bc} have provided
41 an insight into the molecular architecture of this enzyme. By comparing with other metallo-
42 PLC from *Clostridium perfringens* and *Clostridium bifermentans*, this enzyme presents only
43 the N-terminal part 250 residues and truncated of the so-called C-terminal side, conferring
44 sphingomyelin-hydrolyzing, lytic and hemolytic properties to these enzymes [9, 10].
45 Structurally, PC-PLC_{Bc} is composed of eight α -helices, forming a twisted barrel structure [6].
46 PC-PLC_{Bc} is an unusual protein with a trinuclear-zinc center playing a crucial role in the
47 catalytic process, where nine residues (5 His, 2 Asp, 1 Glu, and 1 Trp) are known to be
48 involved in the coordination of zinc ions [11]. Recently, an extracellular nPC-PLC_{Bt} has been
49 purified in our laboratory [12]. Interestingly, this enzyme displayed the highest catalytic
50 activity of about 6000 U.mg⁻¹ using egg PC as the substrate measured at 55-60 °C. nPC-PLC_{Bt}
51 has also the capacity to retain its activity at high temperatures and in alkaline conditions and it

52 has an exclusive capacity to hydrolyze the phosphatidylglycerol (PG) headgroup comparing to
53 the *Bacillus* PC-PLC group [13, 14]. These biochemical criteria suggested that PC-PLC_{Bt}
54 might be suitable for biotransformation in emulsifier production in food industries and as a
55 potential catalyst in industrial oil degumming purposes for the edible oil industry which
56 requires extreme temperatures exceeding the 60 °C. These attractive catalytic and biochemical
57 capacities for industrial processes incite the over-expression of PC-PLC_{Bt} to achieve enough
58 protein amounts. Based on the available literature, several systems have been tried for
59 *Bacillus* PLC gene expression. Among them, the *P. pastoris* system could yield large amounts
60 of the active extracellular enzyme [15], although its cultivation period is relatively long[16].
61 PC-PLC was also overexpressed in *B. subtilis* using a novel expression system [17], but this
62 latter used is due to licensing fees. Ravasi et al. in 2015 reported that high-level production
63 of *B. cereus* PLC could be achieved by using the *C. glutamicum* system [18]. Nevertheless,
64 the mature expression system of *E. coli* remains often the choice allowing a large protein
65 quantity and a high-throughput structural analysis [19]. Although much is known about the
66 function and the structure of the PC-PLC of *Bacillus* group, there remain numerous
67 unanswered questions concerning its kinetic, substrate specificity and interfacial properties
68 towards monomolecular phospholipid films at the air-water interface. The monolayer
69 technique has many advantages. On one hand, it defines the substrate physicochemical state
70 such as the molecular area *via* the interfacial surface pressure. On the other hand, this
71 technique makes possible the investigation of the enzyme capacity to penetrate various
72 phospholipid monolayers at various initial surface pressure [20]. Formerly, kinetic studies of
73 PLC used monomolecular film of radiolabeled phospholipids [21]. However, such approach
74 suffers from the DAG accumulation provoking a variation in the monolayer lipid composition
75 and a decrease in the phospholipid surface density [22]. To avoid these constraints, an
76 alternative monolayer procedure previously adopted for studying the interfacial behavior of

77 PLC activity from *C. perfringens* α toxin [22] was developed. This new approach consists of
78 rapid hydrolysis, by a lipase, of DAG molecules generated from the PLC action on
79 phospholipid films into fatty acid and 2-monoacylglycerol (2-MAG), which are then desorbed
80 from the lipid interface.

81 In the present investigation, a high-level expression of the rPC-PLC_{Bt} in the *E. coli* system is
82 reported. Since the *Bacillus* PC-PLC interfacial behavior has not been investigated yet, we are
83 establishing a comparative monolayer study between the nPC-PLC_{Bt} and the rPC-PLC_{Bt}
84 enzymes, based on a new coupled reaction between the PLC and a strict lipase unable to
85 hydrolyze phospholipid films. Furthermore, new insights into the affinity of PC-PLC_{Bt} for
86 biomembrane are given, in correlation with its interfacial capacity to hydrolyze phospholipid
87 monolayers at high surface pressure.

88

89 **2. Material and methods**

90 **2.1. Chemicals and lipids**

91 Benzamidine was from Fluka (Buchs, Switzerland), tryptone, yeast extract, sodium
92 deoxycholic acid (NaDOC), ethylene diamine tetra-acetic acid (EDTA), β -cyclodextrin (β -
93 CD), and Egg PC (99% purity) were purchased from Sigma Aldrich (St. Quentin Fallavier,
94 France). Isopropyl Thio-D-galactopyranoside (IPTG) was purchased from Boehringer.
95 Marker proteins and Ni-NTA (nickel nitriloacetic acid) resin for affinity chromatography used
96 for enzyme purification were obtained from Bio-Rad. DLPC, DLPE, PG, and PS were
97 purchased from Avanti Polar Lipids. Pure lipid solutions were prepared by adding a volume
98 of chloroform to a known mass of dry sample to obtain the desired concentration.

99 **2.2. Bacterial strains and plasmids**

100 *E. coli* strain Top 10 was used for cloning the gene encoding PC-PLC_{Bt}. *E. coli* strain BL21
101 (DE3) served as the expression host for the rPC-PLC_{Bt} gene construct. The pGEM-T Easy and
102 pET 28b (+) plasmids were used as cloning and expression vectors, respectively. *E. coli*
103 strains were grown in Lysogeny broth (LB) medium, supplemented with 100 $\mu\text{g}\cdot\text{mL}^{-1}$
104 ampicillin or 100 $\mu\text{g}\cdot\text{mL}^{-1}$ kanamycin according to the used plasmid. Restriction
105 endonucleases were from New England BioLabs, wizard PCR preps DNA purification
106 system, and midi-prep kit were bought from Macherey-Nagel, and oligonucleotides were
107 synthesized by Eurofins.

108 **2.3. Proteins**

109 nPC-PLC_{Bt} was purified previously according to our described procedure [12]. The pure
110 native enzyme consists of a single polypeptide chain with a molecular mass of about 28 kDa
111 and specific activity of about 6000 U. mg^{-1} measured at 60 °C °C and pH 8 using pure egg PC
112 as the substrate in presence of 0.5 mM Mg²⁺. Recombinant *Serratia* sp. W3 lipase (rSmL) was
113 overproduced in *E. coli* BL21 and purified in the laboratory as previously described [23].

114 Protein concentrations were determined routinely using the Bradford method [24] with dye
115 reagent and bovine serum albumin as the standard. Sodium dodecyl sulfate-polyacrylamide
116 gel electrophoresis (SDS-PAGE) was performed adopting the procedure of Laemmli [25].

117 **2.4. Molecular cloning of rPC-PLC_{Bt}**

118 The gene part encoding the mature PLC_{Bt} was amplified by PCR from genomic DNA of *B.*
119 *thuringiensis* IL14 using the following primers 5'-ATCGCATATGTGGTCTG
120 CTGAAGATAAACAT-3' and 5'-TACGGGCGGCCGCTTAACGATCTCCGTA CGTATC-
121 3'. The primers were predicted from the N-terminal sequence of the purified nPC-PLC_{Bt} [12]
122 and the C-terminal sequence of the *Bacillus* PLC group. PCR reaction was performed in 50
123 µL reaction mixtures containing 25 pmol of each primer, 0.5 U of Q5®High-Fidelity DNA
124 Polymerase with its adequate buffer (New England Biolabs), 2 mM dNTP mix, and 25 ng
125 DNA as a template. The PCR protocol consisted of 30 cycles at 98°C (30 s), 40°C (30 s),
126 72°C (60 s) respectively and a final extension at 72°C for 10 min. The amplicon (700 bp) was
127 first cloned into pGEM-T Easy, sequenced, excised with *NdeI* and *NotI*, then cloned into the
128 expression pET-28b(+) vector (Invitrogen). The ligation reaction was set in the ratio of 1:1
129 (insert: vector). Competent *E. coli* Top10 cells were transformed with the ligation mixture and
130 transformants were selected on LB plates supplemented with kanamycin at a final
131 concentration of 100 µg.mL⁻¹. The presence of the appropriate insert was determined by
132 colony PCR. The NCBI BLAST and FASTA programs were used for homology searches in
133 the GenBank and Swiss-Prot databases.

134 **2.5. rPC-PLC_{Bt} expression and purification**

135 The *E. coli* BL21 (DE3) strains to contain the different recombinant plasmids were grown at
136 37°C in a 50 mL LB medium containing 100 µg.mL⁻¹ Kanamycin. 0.5 mM IPTG was added
137 to the medium, upon reaching the exponential growth phase, and the cultures were incubated
138 at 23°C for 12 h. Cells were harvested by centrifugation at 3500 × g for 10 min and washed

139 twice with buffer A (20 mM Tris-HCl, pH 8.5, 20 mM NaCl). Cells collected by
140 centrifugation were resuspended in buffer A and were disrupted by sonication using an MSE
141 Sonyprep 150 at full power; 15 s on 15 s off for 15 cycles at 4°C. Cell debris was then
142 removed by centrifugation at $9500 \times g$ for 20 min and the supernatant was assayed for PLC
143 activity. The resulting sample was subjected to a Ni-NTA affinity chromatography
144 substantially equilibrated with buffer A supplemented with 2 mM benzamidine and rPC-
145 PLC_{Bt} was then eluted with an imidazole gradient. The active fractions were then pooled,
146 concentrated, and further purified using Sephadex G-75 column (2.5 cm×150 cm), pre-
147 equilibrated with 25 mM Tris-HCl buffer (pH 8).

148 **2.6. PC-PLC_{Bt} assay**

149 The PC-PLC_{Bt} activity was checked titrimetrically at pH 8.5 and 55°C with a pH-stat using
150 Egg PC as a substrate in the presence of 7 mM NaDOC [12]. Under standard conditions, one
151 unit of the PLC activity corresponds to 1 μmol of PC liberated per minute.

152 **2.7. Biochemical characterization of rPC-PLC_{Bt}**

153 To check the effect of the recombination process on the biochemical characteristics of the
154 rPC-PLC_{Bt}, this enzyme was characterized and compared with the native one. The effect of
155 pH and temperature on the rPC-PLC_{Bt} activity was determined by measuring continuously the
156 PLC activity over the pH range of 7-10 and the temperature range of 20 to 70 °C using an egg
157 PC emulsion. The enzyme pH stability was measured by incubating the enzyme in different
158 pH values (3-12) using the corresponding buffers at a final concentration of 100 mM. The
159 residual activity was determined after incubation at room temperature for 2 h. The thermal
160 stability was determined by incubating the enzyme solution at different temperatures (20-
161 60°C) and pH 8.5 for 1 h. The rPC-PLC_{Bt} residual activity was determined after centrifugation
162 to remove the denatured enzyme fraction under optimal assay conditions. The effect of

163 NaDOC and metal ions on enzyme activity was also checked at increasing concentrations
164 under predicted optimal conditions using Egg PC as the substrate.

165 **2.8. Monitoring reaction rates using monomolecular film technique**

166 *2.8.1. Monolayer measurements*

167 Measurements were performed with KSV-2200 Baro-stat equipment (KSV-Helsinki). The
168 principle of the method was described elsewhere [26]. A zero-order trough with two
169 compartments, a reservoir compartment 14.8×24.9 cm in size, and a reaction compartment in
170 which the enzymes were injected (total volume 130 mL; total surface area 120 cm^2)
171 connected by a small surface channel was used in this study [27]. A thin platinum plate
172 immersed in the surface of the aqueous phase is attached to an electro-microbalance for
173 measuring the surface pressure (π). A mobile barrier, automatically driven by the barostat,
174 moves over the reservoir compartment to maintain the surface pressure constant and to
175 compensate for the substrate molecules removed from the lipidic film by enzyme hydrolysis.
176 All experiments were performed at room temperature ($25 \text{ }^\circ\text{C}$). The subphase of the reaction
177 compartment was continuously stirred with two magnetic stirrers (250 rpm) and the enzyme
178 solution was injected with a Hamilton syringe only when the phospholipid film covered both
179 compartments. The following buffer was used throughout the experiments: 10 mM Tris-HCl
180 buffer, pH 8.0, 21 mM CaCl_2 , 150 mM NaCl, 1 mM EDTA.

181 **2.8.2. Two enzymatic steps to measure PC-PLC_{Bt} activity on phospholipid monolayer**

182 The enzymatic activities of the PC-PLC_{Bt} were investigated with various phospholipids
183 monolayers using a coupled assay as described by Moreau et al [22]. The principle of this
184 assay is shown schematically in **Figure 1**. The assay involves coupling the PLC catalytic
185 reaction, using a phospholipid monolayer as the first substrate, with the subsequent hydrolysis
186 of the formed DAG by a lipase. This method requires a lipase that is not able to hydrolyze
187 phospholipid monolayer such as rSmL according to our previous report [28].

188 The phospholipid solution was spread, with a Hamilton syringe, into a clean air/water
189 interface. The monomolecular film was maintained at constant surface pressure. Initially,
190 rSmL was added to the aqueous subphase and no activity was detected. When PC-PLC_{Bt} was
191 injected into the reaction compartment, the reaction was started as reflected by the mobile
192 barrier movement back and forth over the reservoir. PLC hydrolyzed the insoluble
193 phospholipid films generating a stable 1,2-DAG film and water-soluble phosphocholine. The
194 1,2-DAG, in contrast to phospholipid film, was subsequently hydrolyzed by the rSmL
195 ultimately producing the 2-MAG and free fatty acid. These enzyme-catalyzed reaction
196 products were rapidly desorbed from the interface in the form of complexes with β -CD
197 allowing a constant surface pressure. Specific activities were expressed as the number of
198 moles of the substrate hydrolyzed per unit time and per unit surface ($\text{mol}\cdot\text{cm}^{-2}\cdot\text{min}^{-1}$) of the
199 reaction compartment of the “zero-order” trough for an arbitrary PLC concentration of 1M.

200 **2.9. Hemolysis assay**

201 The hemolytic activity of the rPC-PLC_{Bt} was performed using the direct hemolytic test.
202 Freshly collected blood human erythrocytes were immediately mixed with drops of heparin (5
203 $\text{mg}\cdot\text{mL}^{-1}$), to prevent blood coagulation. In the first step, the suspension is centrifuged at 780
204 $\times g$ for 15 min to eliminate the serum and the obtained pellet undergoes three successive
205 washes with 0.9% NaCl, each of which is followed by gentle centrifugation at 780 $\times g$ for 15
206 min. Recovered erythrocytes were suspended in phosphate-buffered saline (PBS pH 7.4) and
207 centrifuged at 970 $\times g$ for 5 min at 4°C to obtain a pure suspension of erythrocytes. The
208 supernatant and buffy coats were removed by gentle aspiration, and the above process was
209 repeated two more times. Finally, pure erythrocytes were suspended in PBS to make 1%
210 solution for the hemolytic assay and various concentrations of pure rPC-PLC_{Bt} were added to
211 red blood cells suspension. The rPC-PLC/erythrocyte mixture was incubated at 37°C for 30
212 min and then centrifuged at 970 $\times g$ for 5 min at 4°C. The absorbance of the supernatants was

213 determined at 545 nm to measure the extent of red blood cell lysis and hemoglobin release. In
214 parallel, erythrocytes were incubated in PBS containing 1% Triton X-100 (100% hemolysis)
215 and PBS alone (0% hemolysis), which will serve as a positive and negative control,
216 respectively.

217 **2.10. Cell Culture**

218 Primary chondrocytes were obtained from newborn (4-6 days) SWISS mice by successive
219 enzymatic digestion of knee and femoral head cartilage [29]. Cells were cultured for 7 days in
220 Dulbecco's modified Eagle medium (DMEM) supplemented with 10% (v:v) FBS, penicillin
221 ($100 \text{ U}\cdot\text{mL}^{-1}$), and streptomycin ($0.1 \text{ mg}\cdot\text{mL}^{-1}$). The medium was changed every 2-3 days.
222 Non-tumor human prostatic cell line WPMY-1 was purchased from ATCC (Manassas, USA).
223 Human prostate cancer bone metastasis-derived cell line PC-3 was purchased from DSMZ
224 (Braunschweig, Germany). WPMY-1 cells were cultured in DMEM supplemented with 10 %
225 (v:v) FBS and antibiotics. The PC-3 cell line was cultured in Roswell Park Memorial Institute
226 (RPMI) medium supplemented with 10 % (v:v) FBS and antibiotics. Prostatic cell lines were
227 maintained in a humidified atmosphere (5% CO_2) at 37 °C and passaged twice a week. They
228 were weekly monitored by the following tests: morphology check by visual inspection,
229 growth curve analysis, and mycoplasma detection (Mycoplasma detection kit; InvivoGen,
230 California, USA). All experiments were started with low-passaged cells (<20 times).

231 **2.11 Cell viability and cytotoxicity assays**

232 The number of viable cells was determined using the MTT assay, which is based on the
233 reaction of a yellow tetrazolium salt with cellular dehydrogenases to form purple formazan
234 crystals [30]. Cells ($3 \times 10^4 \text{ cells}/\text{cm}^2$ for murine chondrocytes, $2 \times 10^4 \text{ cells}/\text{cm}^2$ for WPMY-1
235 cells and $10^4 \text{ cells}/\text{cm}^2$ for PC-3 cells, respectively) were seeded in 12-well plates. Cells were
236 treated a week later (chondrocytes) or after 72 h with increasing concentrations of rPC-PLC_{Bt}
237 ($0.05\text{-}0.2 \text{ mg}\cdot\text{mL}^{-1}$) during 72 h. MTT was then added at a final concentration of 0.125 g/L.

238 The plate was further incubated for 4 h at 37°C, after which the culture medium was removed,
239 and the formed formazan crystals were dissolved in 1 mL of DMSO. After 30 min incubation,
240 the absorbance of the plate was measured at 570 nm on an Infinite-M200 pro Plate reader
241 (TECAN, Männedorf, Switzerland). Results were expressed as mean \pm standard deviation of
242 three independent experiments.

243 The cytotoxic effect of rPC-PLC_{Bt} treatment was assessed using the Lactate Dehydrogenase
244 (LDH) assay that relies on the detection of a cytosolic enzyme, the LDH, in the culture
245 medium as an indicator of membrane disruption after cell death. Cells were seeded in 12-well
246 plates and treated as described previously. LDH was detected in 50 μ L of culture medium
247 using an LDH Cytotoxicity Assay Kit (Sigma-Aldrich), as described by the manufacturer.
248 Results were expressed as mean \pm standard deviation of three independent experiments.

249 **2.12. Modeling, Molecular dynamic (MD) simulation, and MM/PBSA calculation**

250 As no crystal structures were available for PC-PLC from *Bacillus thuringiensis*, molecular
251 modeling has been performed. Briefly, a BLAST search [31] performed against the Protein
252 Data Bank [32] identified PDB ID 1AH7 [6], PC-PLC from *Bacillus cereus*, as a template
253 (99.6% identity on 245 residues). The reconstruction of the three-dimensional (3D) models
254 was carried out by substitution and reorientation of the substituted amino acid (S188P) using
255 the COOT program [33]. After this step, the structure was energy minimized, computations
256 being done in *vacua* by using the GROMOS96 43B1 parameters set [34]. Docking of a 1,2-
257 diacyl-*sn*-phosphoglycerol (PG) into the PC-PLC_{Bt} model structure was performed using
258 AutoDockVina embedded in PyRx 0.8 [35, 36]. Briefly, the protein structure was prepared for
259 docking by removing unwanted water molecules and bound ligands and by adding polar
260 hydrogens atoms using Discovery Studio Visualizer. The same program was used to build the
261 substrates molecules as PDB files and for energy minimization. PyRx was used for converting
262 all molecules to AutoDock Ligand format (PDBQT). The three-dimensional grid box for

263 molecular docking simulation was obtained using Autodock tools. The Grid box was centered
264 to cover the active site and all essential residues. The docking results were analyzed by
265 comparing the binding interactions and binding energies between substrate molecules and the
266 enzyme.

267 To give a better binding energy approximation of the PG/PLC and PC/PLC complexes,
268 MM/PBSA approximation was realized using YASARA Structure. First, the
269 phospholipid/PLC_{Bt} complex structure was filled with water and cell neutralization was
270 performed. MD simulation was started at 303 K, with Amber14 force-field, and ran for 20 ns.
271 Simulation snapshots were saved every 100 ps for MM/PBSA calculation. For each
272 simulation snapshot, binding energy was calculated as the difference between the sum of
273 potential and solvation energies of the separated compounds and the sum of potential and
274 solvation energies of the complex. Because the entropy term from normal mode analysis is
275 missing, we get almost 'MM/PBSA' via binding energy average from all snapshots.

276

277 3. Results and discussion

278 3.1. Molecular cloning and expression of rPC-PLC_{Bt}

279 The PCR product corresponding to the gene part encoding the mature PC-PLC_{Bt} sequence
280 length was 735 bp encoding 246 amino-acids including the first methionine inserted (**Figure**
281 **S1**). The catalytic triad active site residues E₄, Y₅₆, and F₆₆ could be identified (**Figure S1**).
282 The rPC-PLC_{Bt} protein sequence shows an identity of 99 % with the PC-PLC_{Bc} already
283 reported and predicted [37-39] through comparison with the protein sequences of *Bacillus*
284 group PLC produced and crystallized [6], in addition to the first methionine inserted, one
285 substitution (S188P) is noted (**Figure S1**). Expression of rPC-PLC_{Bt} was performed in *E. coli*
286 BL21 (DE3). The medium composition, the inducer concentration, and the induction
287 temperature for optimum enzyme production by *E. coli* BL21 were optimized using the
288 classical method 'one variable at a time'. In the light of the obtained results, we could
289 conclude that by decreasing the incubation temperature to 23°C and IPTG concentration to
290 0.5 mM, the enzyme production was oriented towards the intracellular medium underactive
291 form reaching 24000 U.L⁻¹ of culture. The enzyme activity was observed to start soon after
292 induction and reached its optimum after 12 h of induction; in addition, the results show that
293 the LB medium is more adequate allowing the best level of activity. At 37 °C, rPC-PLC_{Bt} was
294 found to agglomerate in the inclusion bodies [40]. Based on the available literature the
295 expression of PLC from bacillus can lead to two voices: intracellular expression in an inactive
296 form, and extracellular expression in the native form [3]. *E. coli* host is often the choice for a
297 large amount of inclusion bodies, which could only be converted into an active protein by a
298 lengthy protocol with low yields [41]. In this report we have interestingly succeeded, by
299 optimization of the induction conditions, to overexpress the mature PC-PLC from *Bacillus*
300 *thuringiensis* in an active soluble form in the *E.coli* system, avoiding thus the tedious
301 refolding steps.

302 **3.2 Purification and biochemical characterization of rPC-PLC_{Bt}**

303 The purification of rPC-PLC_{Bt} was performed using a Ni-NTA affinity column. The protein
304 was eluted by a linear imidazole gradient at around 50 mM, as an inactive form under the
305 imidazole effect (**Figure 2A**). Protein fractions were collected, concentrated, and
306 subsequently filtrated using Sephadex G-75 gel filtration column to get rid of any imidazole
307 traces susceptible to influence the pure recombinant enzyme stability (**Figure 2B**). Active
308 fractions analysis by SDS-PAGE reveals the presence of the rPC-PLC_{Bt} as a pure protein band
309 of about 28 kDa (**Figure 2B**). From 250 mL of culture medium, about 3.5 mg of pure rPC-
310 PLC_{Bt} were obtained with a specific activity of 1372 U.mg⁻¹. This protein amount has never
311 been obtained from the wild *B. thuringiensis IL14* allowing only 0.83 mg of nPC-PLC_{Bt} [12].
312 It should be noted that this rPC-PLC_{Bt} amount is expected since it was previously reported
313 that when the PC-PLC expression is controlled under the strong T7 promoter, a higher protein
314 amount can be produced in this recombinant system than in *B. thuringiensis* [41].
315 In our previous study [12], three metal ions (Mg²⁺, Ca²⁺, and Zn²⁺) were reported as nPC-
316 PLC_{Bt} activators. Thus, we tested the effect of these metal ions on the recombinant form
317 activity under the same optimal conditions used for the wild-type form. From **Figure 3A**, we
318 were able to confirm that Ca²⁺, Zn²⁺ and Mg²⁺ are phospholipase activity stimulators and zinc
319 ions are shown to be the most effective on the activity of rPC-PLC_{Bt}. The presence of only 0.1
320 mM of Zn²⁺ in the assay medium induces an increase of the rPC-PLC_{Bt} activity 5 times as
321 compared to twice for nPC-PLC_{Bt} [12]. However, an excessive Zn²⁺ concentration in the assay
322 medium begets a rollback in the phospholipase activity which comes in agreement with
323 findings published by Lyu et al., 2016. The latter reported that although the metallo-character
324 of PC-PLC_{Bc}, when expressed in *P. pastoris* X-33 its activity is inhibited beyond 5 mM Zn²⁺
325 [3]. Concerning the detergent effect, rPC-PLC_{Bt} activity was assayed in the presence of
326 increasing concentrations of NaDOC (**Figure 3B**). As previously described for the native

327 form, rPC-PLC_{Bt} is still always characterized as a surfactant enzyme since it showed the
328 highest specific activity at 7 mM NaDOC and beyond this concentration, the NaDOC does not
329 exert any inhibitory effect [12]. Indeed, as well explained [42, 43], this surfactant is involved
330 in the solubilization of phospholipids or the DAG hydrolysis product. The effect of pH and
331 temperature on the rPC-PLC_{Bt} activity was investigated and our findings prove that the
332 expression process kept the thermo-activity character of the native enzyme [12]. As it could
333 be seen from **Figure 3C**, the rPC-PLC_{Bt} displays its optimal hydrolytic activity of about 1372
334 U.mg⁻¹ at 60 °C which is 7 times higher than when the enzyme is incubated at room
335 temperature. Such characteristic is one of the most sought-after criteria, for an industrial
336 application because the realization of enzymatic process at high temperature offers many
337 advantages [44, 45]. Furthermore, rPC-PLC_{Bt} activity was measured at 60 °C at different pH
338 values using egg PC dispersion as substrate. The pH vs activity profile (**Figure 3D**)
339 demonstrates that rPC-PLC_{Bt} is active in a pH range from 7.5 to 9.5 with an optimum reached
340 at pH 8. On both sides of this pH zone, the activity starts to decrease contrary to an
341 overexpressed PC-PLC_{Bc} in *P. pastoris* X-33 presenting the optimal activity under mildly
342 acidic conditions (pH 4-5) [3]. Unlike published findings for nPC-PLC_{Bt} [12], the thermal and
343 pH stability of the rPC-PLC_{Bt} were affected by the presence of zinc ions in the reaction
344 medium. In fact, from the thermo-stability profile of the enzyme (**Figure 3E**), we conclude
345 that rPC-PLC_{Bt} retained around 60% of its initial activity after incubation for 1 h at 65 °C in
346 the presence of 0.1 mM zinc ions compared to only 35% of remaining activity in the absence
347 of zinc ions. Furthermore, the rPC-PLC_{Bt} shares the same stability profile as the native form
348 [12] where rPC-PLC_{Bt} keeps the full initial activity after incubating the enzyme at various pH
349 values (from 6 to 8.5) for 1 h (**Figure 3F**). However, on both sides of this range, the activity
350 decreased slightly since rPC-PLC_{Bt} retained 70% and 50% of its initial activity when
351 incubating the enzyme at pH 5 and pH 10, respectively for 1h (**Figure 3F**). This weak

352 stability could be caught up by the presence of the zinc ions in the reaction medium, which
353 can restore a stability profile like the native form. Therefore, when adding 0.1 mM Zn²⁺, rPC-
354 PLC_{Bt} keeps 70% and 50% of its initial activity at pH 4 and at pH 12, respectively (**Figure**
355 **3F**). The experiment was extended up to 3 hours and interestingly, the recombinant enzyme
356 remains stable within a pH range of 6-8 where nearly 90% of residual activity was recorded.
357 The presence of zinc ions allows more than 55% of rPC-PLC_{Bt} activity at pH 4 and 11 after 3
358 h. Consequently, it appears that the presence of zinc ions induces conformational changes
359 which involve a significant modification in the secondary structure of PC-PLC_{Bt} leading to its
360 stability and to the improvement of its catalytic properties. In that context, it was reported that
361 the complexed Zn²⁺ forms a key bond with the E₁₄₆ residue in the active site of PC-PLC_{Bc}
362 indispensable for the stabilization of the secondary and tertiary conformation of the enzyme
363 [40]. It appears that E₁₄₆ in PC-PLC_{Bc} serves as an essential ligand for Zn²⁺. Mutation at this
364 position generates an enzyme with reduced thermostability which binds only two zinc ions
365 rather than three compared to wild-type PC-PLC_{Bc} [46].

366 As it was mentioned above, by comparing the PC-PLC_{Bt} with the protein sequences of the
367 *Bacillus* PLC group already produced and expressed, a substitution of S₁₈₈ in PC-PLC_{Bc} by
368 P₁₈₈ in PC-PLC_{Bt} was noted. This finding led us to conceive the hypothesis that this mutation
369 is at the origin of the major differences, including thermostability and thermoactivity, between
370 the PC-PLC_{Bt} and that of *B. cereus*. The molecular model of PC-PLC_{Bt} (**Figure 4A**) shows
371 that mutation S188P occurs in between the two helices αF and αG. Consequently, this proline,
372 considering its particular geometric properties, may block the hinge (between residues 187
373 and 192) allowing the structure to "bend" in *B. cereus*. Another hinge (hinge 2 in **Figure 4A**),
374 between helices αH1 and αH2, can be located at P218. These 2 hinges would therefore allow
375 certain flexibility to this part of PC-PLC_{Bc} (helices αG and αH1) and considering long-
376 distance interactions, even flexibility to helix αE (**Figure 4B**). Conversely, for thermostable

377 enzymes, an increase in rigidity is generally observed (notably due to an increased proline
378 number). The S188P mutation, therefore, goes exactly in this direction since PC-PLC_{Bt} is
379 shown to be more thermostable than PC-PLC_{Bc}.

380 Even though it cannot be excluded that the structural bases responsible for thermostability and
381 pH stability may be located elsewhere in the 3D structure of the enzyme. The rPC-PLC_{Bt}
382 used, due to a different amino-terminal extremity (presence of an extra methionine, see
383 **Figure S1**), may adopt a different conformation and display different structural properties,
384 especially concerning thermostability, and so “cancel” the consequences of the S188P
385 mutation.

386 **3.3. Kinetic measurements of rPC-PLC_{Bt} activity at the monolayer interface: Influence** 387 **of Film Pressure and Substrate Specificity**

388 The DAG generated under PLC-catalyzed of phospholipid film was subsequently hydrolyzed
389 by the rSmL (**Figure 1**). Initially, the addition of the rSmL underneath the phospholipid's
390 monolayer was not followed by any detectable change in surface pressure. This indicates that
391 no significant penetration of lipase and no hydrolysis of the phospholipid film by the rSmL
392 were detected since phospholipids are not substrates for rSmL according to our previous
393 report [28]. Ten minutes later, pure PC-PLC_{Bt} was then injected and the enzymatic activity as
394 reflected by the barrier movement of the barostat was recorded continuously at constant
395 surface pressure. It should be noted that the PLC activity was measured as a function of the
396 rSmL amount, ranging from 0 to 50 ng. When no lipase is added, no advancement of barostat
397 barrier is registered then the hydrolysis rates were linear with the rSmL amount up to around
398 20 ng above which remained constant (data not shown). Therefore, in all subsequent
399 experiments, a final rSmL amount of 40 ng was selected to measure the PC-PLC_{Bt} activity on
400 monolayers of four phospholipids (DLPC, DLPE, PG, and PS). Besides, when adding PC-
401 PLC_{Bt}, enzymatic activity was not detected until after a certain time that corresponds to the

402 lag period indicative of a presteady state, according to the literature it corresponds to the time
403 required for the diffusion of the enzyme from the subphase to the interface and its adsorption
404 to the phospholipid monolayer [47, 48]. After the latency period, the surface pressure
405 increases abruptly (data not shown) until a maximum level confirming the lag-burst behavior
406 previously described by He and Li for PLC [49] and PLA₂ [50, 51]. According to BAM and
407 PMIRRAS experiments, this sharp increase in surface pressure is due to the molecular
408 reorganization of the hydrolysis product (DAG) [47, 52].

409 The rate of hydrolysis of phospholipid films by the native and the recombinant PC-PLC_{Bt}
410 forms was plotted as a function of the surface pressure and results showed bell-shaped curves
411 with the four phospholipids (DLPC, DLPE, PG, PS) tested as substrates (**Figure 5**). By
412 focusing on the surface pressure, whatever the native or the recombinant forms, a lack of PLC
413 activity was noted at low surface pressures (below 10 mN.m⁻¹). This irreversible interfacial
414 denaturation of the enzyme at low surface pressures (corresponding to high interfacial tension
415 and energy levels) can be prevented by increasing the surface pressure (thus lowering the
416 interfacial tension), either by adding amphiphiles such as bile salts or proteins or by
417 compressing the monomolecular films mechanically [53, 54]. PLC activity increased
418 continuously by surface pressure rise until reaching the highest enzyme activities on DLPC,
419 DLPE, PG, and PS headgroups at surface pressures of 15 and 25, 20, and 25 mN.m⁻¹,
420 respectively (**Figure 5**). However, the hydrolysis rates are negligible at surface pressure
421 superior to 30 mN.m⁻¹. This low PC-PLC_{Bt} activity is due to a decrease of SmL adsorption to
422 phospholipid monolayer above 31 mN.m⁻¹ as previously reported [23]. Similar results were
423 found by Moreau et al [22], who reported that the *C. perferingens* PLC activity decreased
424 sharply around a threshold surface pressure of about 17 mN.m⁻¹ using 1,2-didodecanoyl-*sn*-
425 glycerol-3-phosphocholine and 1,2-dilauroyl-*sn*-glycerol-3-phosphocholine films however no
426 hydrolysis was detected when PE, PS, or PG films were used as substrates [22]. In addition,

427 even with varying hydrolysis efficacy, the enzymatic activity could be detected for all the
428 substrates tested. It is worth noticing that heterologous expression did not affect the substrate
429 specificity of the PC-PLC_{Bt} since the nPC-PLC_{Bt} hydrolyze more efficiently all the
430 phospholipids compared to the recombinant enzyme (**Figure 5**). Indeed, at optimum surface
431 pressures, the maximum specific activities of nPC-PLC_{Bt} on DLPC, DLPE, PG, and PS
432 headgroups were 125 (**Figure 5A**), 86 (**Figure 5B**), 58 (**Figure 5C**), and 30 mole.cm⁻².min⁻¹.mg⁻¹
433 (**Figure 5D**), respectively, while the maximum specific activities of rPC-PLC_{Bt} on the
434 same substrates were shown to be 40 (**Figure 5A**), 30 (**Figure 5B**), 8.5 (**Figure 5C**) and 7.5
435 mole.cm⁻².min⁻¹.mg⁻¹ (**Figure 5D**), respectively. According to our forecasts, we suggest that
436 this difference is due to the addition of the first M residue start codon upstream of W residue
437 in the recombinant construction comparing to the native form where the W residue was
438 identified by the NH₂ terminal sequence as the first residue [12]. Indeed, it was published for
439 the PC-PLC_{Bc} [3] that the initial amino acid is widely considered as indispensable for enzyme
440 activity. Indeed, this first W residue contributes to the coordination with the essential zinc
441 ions [41, 55] and when it was exposed, a sharp increase in the activity is noted. Besides, this
442 activity decrease could be explained by the fact that the recombinant enzyme wasn't properly
443 folded in the *E. coli* system, as in the wild strain. Furthermore, the ability of both PC-PLC_{Bt}
444 forms to hydrolyze the PG (**Figure 5D**), more pronounced for the native form, remains
445 exclusive compared to all *Bacillus* PLC published [13, 56]. Because mutation S188P is
446 located far from the catalytic site (**Figure 4B**) and does not appear to alter the overall tertiary
447 structure of the enzyme (data not shown), exclusive capacity to hydrolyze the PG substrate
448 must be due to subtle steric and/or electronic perturbations in the substrate-binding pocket.
449 The altered dynamic motion of helices αE , αG , and $\alpha H1$ due to P188 (**Figure 4B**) may induce
450 conformational changes or differences in hydration network in the active site and so be
451 responsible for enhanced affinity for PG headgroup in PC-PLC_{Bt}. Indeed, results from

452 MM/PBSA evaluation (**Figure 4C and 4D**) show that the mutation S188P seems to enhance
453 affinity for PG as its binding energy is increased by almost 40% (difference of 236.75 kJ/mol
454 between PC-PLC_{Bc} and PC-PLC_{Bt}). On the contrary, the affinity for PC is not altered by the
455 mutation since the difference concerning its binding energy is shown to be only 14.85 kJ/mol
456 (corresponding to the energy of one hydrogen bond) between *B. cereus* and *B. thuringiensis*
457 enzyme. The capacity of the PC-PLCs to efficiently hydrolyze PE and PC two of the most
458 abundant phospholipids present in vegetable oils [57], the large amount of enzyme produced,
459 and the significant stability at high temperatures present this new phospholipase in the hot
460 spot for oil enzymatic degumming allowing a higher yield of oil, both by generating 1,2-
461 diacylglycerol (DAG) from phospholipids and by releasing the trapped TAGs following the
462 reduction of gums volume [18, 58].

463 **3.4. Hemolytic activity and cytotoxic potential of rPC-PLC_{Bt}**

464 Biomembranes provide a dynamic and complex environment for biological reactions [59]. In
465 the erythrocyte membrane, PC and sphingomyelin-containing choline are mainly located in
466 the outer monolayer while aminophospholipid, including PS and DLPE, are enriched in the
467 cytoplasmic leaflet of the membrane [59]. Several studies highlighted evidence of a
468 correlation between the kinetic properties of phospholipases and their efficient attack of
469 biological membranes. For example, Saikia *et al.* [60] demonstrated the link between catalytic
470 and erythrocytes membrane damaging activities of an acidic PLA2 purified from *Daboia*
471 *russelli* venom. Moreover, marine snail digestive [61] and venom glands *Scorpio maurus*
472 phospholipases [62] were found to exhibit hemolytic activity towards erythrocytes which
473 could be related to their ability to interact with phospholipid monolayer at high surface
474 pressure. In our report, given the prominent catalytic power of the PC-PLC_{Bt} and the great
475 abilities to bind and hydrolyze phospholipid monolayers at high surface pressure, we aimed to
476 investigate the individual cytotoxic potential of pure rPC-PLC_{Bt} on mammalian cells.

477 Initially, the hemolytic activity of the PC-PLC_{Bt} was measured with various concentrations
478 using rat erythrocytes as a model for membranes. As can be seen from **Figure 6A**, the rPC-
479 PLC_{Bt} exhibits a prominent direct hemolytic power since it was shown able to lyse all the
480 erythrocytes at 200 µg.mL⁻¹ after only 30 min at 37°C. Indeed regarding the hemolytic
481 power, it is noted that there is a divergence in the bibliography between those who reported
482 that the *bacillus* PC-PLC metalloenzyme provides the bacteria with a lecithinase activity but
483 not a hemolytic activity and the induction of hemolytic power is due to an effective hemolytic
484 complex, called cereolysin AB resulting of an enzymatic coupling between sphingomyelinase
485 and PC-PLC [37, 63, 64] and those who published that the *B. cereus* and *C. perfringens* PLCs
486 are talented by a high hemolytic power [65].

487 Considering this ability to disrupt biological membranes, PC-PLC_{Bt} could exhibit a cytotoxic
488 effect in mammals cells. The lytic potential of rPC-PLC_{Bt} was assessed by treating murine
489 primary chondrocytes, human prostatic stromal myofibroblast cell line WPMY-1, and human
490 prostatic metastatic cell line PC-3 with pure rPC-PLC_{Bt} at different concentrations (50-
491 200 µg.mL⁻¹) (**Figure 6B**). The cytotoxicity effect of the PLC is based on the measurement of
492 lactate dehydrogenase (LDH) activity released by damaged cells after cell bursting to rPC-
493 PLC_{Bt} during 72 h. As indicated in Figure 8B, rPC-PLC_{Bt} reduced viability and also induced
494 cytotoxicity on cultured cells in a dose-dependent manner. A linear correlation was observed
495 between cell viability and LDH activity. Overall, rPC-PLC_{Bt} presented high cytotoxic effects
496 on primary chondrocytes, WPMY-1, and PC-3 cells, with cell viability mostly decreasing
497 varying between 60 and 70 % at the highest concentrations (**Figure 6B**). By comparing
498 WPMY-1 with PC-3, it would seem that the decrease in the viability of PC-3 is greater than
499 that of WPMY-1, in particular with the lowest concentration of 50 µg.mL⁻¹ (**Figure 6B**, upper
500 panel). For toxicity, an increase in LDH activity released by damaged cells was noted after the
501 three doses injection for the different lines although the cytotoxic effect is more pronounced

502 in the PC-3 tumor cell line compared to its control line WPMY-1 since even at a reduced dose
503 of $50 \mu\text{g.mL}^{-1}$, approximately 50% of lysed PC-3 tumor cells were detected against 30% for
504 the WPMY-1 cells (**Figure 6B**, bottom panel).

505 This bacterial rPC-PLC_{Bt} great lytic power could be attributed to the DAG released
506 subsequent of the action of the rPC-PLC_{Bt} on membrane phospholipids which disturbs firstly
507 the properties of the biophysical membrane, especially the fluidity, the charge, and the
508 permeability [66, 67], with a possibility of interaction with cytosolic proteins inducing spatial
509 reorganization signaling complexes leading to the affection of cellular processes [68]. Indeed
510 bacterial PLCs have been included among the virulence factors key to bacterial pathogenesis
511 [69] and evidence implicating the Zn^{2+} metalloPC-PLCs in host cell penetration, injury, and
512 lysis by microorganisms has been proved since the inactivation of the PLC-encoding gene
513 impairs the virulence of a pathogen [70-72].

514 **Conclusions**

515 Successful production of soluble active is reported when express the PC-PLC from *B.*
516 *thuringiensis* in the *E coli* host avoiding thus time-consuming refolding step. The specific
517 activity of the pure rPC-PLC_{Bt} was around 1372 U.mg⁻¹ measured at 60 °C on a PC emulsion
518 in the presence of 0.1 mM Zn²⁺. Purified phospholipase kept at almost, its biochemical
519 properties with an improvement of the Zn²⁺ role required for catalysis and maintaining of the
520 rPC-PLC_{Bt} structure. The high expression yield and the excellent thermophilic properties are
521 valuable features for this rPC-PLC_{Bt} in industrial applications, especially for oil degumming
522 carried out under extreme conditions and offering both economic and environmental benefits.
523 A comparative kinetic study was investigated for the first time with various phospholipids
524 monolayers using a coupled assay. The main conclusions indicate that both native and
525 recombinant PC-PLC_{Bt} forms can hydrolyze phospholipid monolayers with different
526 efficiency and various optimal surface pressures ranging from 15 to 25 mN.m⁻¹. The DLPC is
527 the major hydrolyzed substrate followed by the DLPE however the hydrolysis rate is low with
528 PG and PS. The interesting capacity binding to phospholipid monolayers at high surface
529 pressure is demonstrated correlated to the prominent direct hemolytic power and cytotoxic
530 potential of this rPC-PLC on tumoral mammals cells. New insights on the exact
531 mechanistic aspects of this enzyme's cytotoxicity will be forthcoming soon and exploited for
532 therapeutic and pharmacological purposes as a bactericidal and anti-tumor agent.

533

534 **Fundings:** This work was financially supported by the Tunisian Ministry of Higher Education
535 and Scientific Research through a grant number “18PJEC08-04” and the “PHC-Maghreb”
536 program of the French Ministry of Foreign Affairs and Ministry of Higher Education,
537 Research and Innovation “code Campus France: 43791TM, code PHC: 01MAG20”.

538 **Conflicts of Interest:** The authors declare no conflict of interest.

539 **REFERENCES**

- 540 [1] R.M. Adibhatla, Distinction between phosphatidylcholine (PC)-specific phospholipase C
541 (PC-PLC) and phosphatidylinositol (PI)-specific phospholipase C (PI-PLC) needs clarification,
542 Biochemical and Biophysical Research Communications, 419 (2012) 447; author reply 448-
543 449.
- 544 [2] N. Barton, A new process for degumming: the use of phospholipase C to improve yields
545 during refining of high phosphorus vegetable oils, 99th AOCS Annual Meeting & Expo,
546 Seattle, 2008.
- 547 [3] Y. Lyu, L. Ye, J. Xu, X. Yang, W. Chen, H. Yu, Recent research progress with
548 phospholipase C from *Bacillus cereus*, Biotechnology letters, 38 (2016) 23-31.
- 549 [4] A.J. Dijkstra, Enzymatic degumming, European Journal of Lipid Science and Technology,
550 112 (2010) 1178-1189.
- 551 [5] D. Fu, Y. Ma, W. Wu, X. Zhu, C. Jia, Q. Zhao, C. Zhang, X.Z. Wu, Cell-cycle-dependent
552 PC-PLC regulation by APC/CCdc20-mediated ubiquitin-proteasome pathway, Journal of
553 Cellular Biochemistry, 107 (2009) 686-696.
- 554 [6] E. Hough, L.K. Hansen, B. Birknes, K. Jynge, S. Hansen, A. Hordvik, C. Little, E.
555 Dodson, Z. Derewenda, High-resolution (1.5 Å) crystal structure of phospholipase C from
556 *Bacillus cereus*, Nature, 338 (1989) 357-360.
- 557 [7] T. Johansen, T. Holm, P.H. Guddal, K. Sletten, F.B. Haugli, C. Little, Cloning and
558 sequencing of the gene encoding the phosphatidylcholine-preferring phospholipase C of
559 *Bacillus cereus*, Gene, 65 (1988) 293-304.
- 560 [8] C.L. Franklin, H. Li, S.F. Martin, Design, synthesis, and evaluation of water-soluble
561 phospholipid analogues as inhibitors of phospholipase C from *Bacillus cereus*, The Journal of
562 Organic Chemistry 68 (2003) 7298-7307.
- 563 [9] R.W. Titball, Bacterial phospholipases C, Microbiology and Molecular Biology Reviews,
564 57 (1993) 347-366.
- 565 [10] R.W. Titball, D.L. Leslie, S. Harvey, D. Kelly, Hemolytic and sphingomyelinase
566 activities of *Clostridium perfringens* alpha-toxin are dependent on a domain homologous to
567 that of an enzyme from the human arachidonic acid pathway, Infection and Immunity, 59
568 (1991) 1872-1874.
- 569 [11] P.J. Hergenrother, S.F. Martin, Phosphatidylcholine-preferring phospholipase C from *B.*
570 *cereus*. Function, structure, and mechanism, Bioorganic Chemistry of Biological Signal
571 Transduction, (2000) 131-167.
- 572 [12] A. Eddehech, N. Smichi, Y. Arhab, A. Noiri, A. Abousalham, Y. Gargouri, Z. Zarai,
573 Production, purification and functional characterization of phospholipase C from *Bacillus*
574 *thuringiensis* with high catalytic activity, Process Biochemistry, 83 (2019) 122-130.
- 575 [13] L. Bora, Characterization of novel phospholipase C from *Bacillus licheniformis* MTCC
576 7445 and its application in degumming of vegetable oils, Applied Biochemistry and
577 Microbiology, 49 (2013) 555-561.

- 578 [14] C.G. Wang, M.K. Chen, T. Chen, Improved purification and some properties of a novel
579 phospholipase C from *Bacillus mycoides* strain 970, *African Journal of Microbiology*
580 *Research*, 4 (2010) 396-399.
- 581 [15] C. Elena, P. Ravasi, S. Cerminati, S. Peiru, M.E. Castelli, H.G. Menzella, *Pichia pastoris*
582 engineering for the production of a modified phospholipase C, *J Process Biochemistry*, 51
583 (2016) 1935-1944.
- 584 [16] K.-H. Seo, J.I. Rhee, High-level expression of recombinant phospholipase C from
585 *Bacillus cereus* in *Pichia pastoris* and its characterization, *Biotechnology Letters*, 26 (2004)
586 1475-1479.
- 587 [17] M.A. Durban, J. Silbersack, T. Schweder, F. Schauer, U.T. Bornscheuer, High level
588 expression of a recombinant phospholipase C from *Bacillus cereus* in *Bacillus subtilis*,
589 *Applied microbiology and biotechnology*, 74 (2007) 634-639.
- 590 [18] P. Ravasi, M. Braia, F. Eberhardt, C. Elena, S. Cerminati, S. Peirú, M.E. Castelli, H.G.
591 Menzella, High-level production of *Bacillus cereus* phospholipase C in *Corynebacterium*
592 *glutamicum*, *Journal of Biotechnology*, 216 (2015) 142-148.
- 593 [19] R. Chen, Bacterial expression systems for recombinant protein production: *E. coli* and
594 beyond, *Biotechnology Advances*, 30 (2012) 1102-1107.
- 595 [20] M.B. Ali, R. Jallouli, Y. Gargouri, Y.B. Ali, Evaluation of the recombinant turkey
596 pancreatic lipase phospholipase activity: A monolayer study, *International journal of*
597 *biological macromolecules*, 81 (2015) 349-355.
- 598 [21] S.T. Hernández-Sotomayor, C. De Los Santos-Briones, J.A. Muñoz-Sánchez, V.M.
599 Loyola-Vargas, Kinetic analysis of phospholipase C from *Catharanthus roseus* transformed
600 roots using different assays, *Plant Physiology*, 120 (1999) 1075-1082.
- 601 [22] H. Moreau, G. Pieroni, C. Jolivet-Reynaud, J. Alouf, R. Verger, A new kinetic approach
602 for studying phospholipase C (*Clostridium perfringens*. alpha. toxin) activity on phospholipid
603 monolayers, *Biochemistry*, 27 (1988) 2319-2323.
- 604 [23] A. Eddehech, R. Rahier, N. Smichi, Y. Arhab, A. Noiriél, A. Abousalham, A. Sayari, Z.
605 Zied, Heterologous expression, kinetic characterization and molecular modeling of a new sn-
606 1,3-regioselective triacylglycerol lipase from *Serratia* sp. W3, *Process Biochemistry*, 103
607 (2021).
- 608 [24] M.M. Bradford, A rapid and sensitive method for the quantitation of microgram
609 quantities of protein utilizing the principle of protein-dye binding, *Analytical biochemistry*, 72
610 (1976) 248-254.
- 611 [25] U.K. Laemmli, Cleavage of structural proteins during the assembly of the head of
612 bacteriophage T4, *Nature*, 227 (1970) 680-685.
- 613 [26] F. Pattus, A. Slotboom, G. De Haas, Regulation of phospholipase A2 activity by the
614 lipid-water interface: a monolayer approach, *Biochemistry*, 18 (1979) 2691-2697.
- 615 [27] F. Carrière, Soixante ans de recherche sur la lipolyse enzymatique des corps gras à
616 Marseille, Oléagineux, Corps gras, Lipides, 15 (2008) 196-207.

- 617 [28] A. Eddehech, Z. Zarai, F. Aloui, N. Smichi, A. Noiriél, A. Abousalham, Y. Gargouri,
618 Production, purification and biochemical characterization of a thermoactive, alkaline lipase
619 from a newly isolated *Serratia* sp. W3 Tunisian strain, *International journal of biological*
620 *macromolecules*, 123 (2019) 792-800.
- 621 [29] M. Gosset, F. Berenbaum, S. Thirion, C. Jacques, Primary culture and phenotyping of
622 murine chondrocytes, *Nature Protocols*, 3 (2008) 1253.
- 623 [30] T. Mosmann, Rapid colorimetric assay for cellular growth and survival: application to
624 proliferation and cytotoxicity assays, *Journal of Immunological Methods*, 65 (1983) 55-63.
- 625 [31] S.F. Altschul, T.L. Madden, A.A. Schäffer, J. Zhang, Z. Zhang, W. Miller, D.J. Lipman,
626 Gapped BLAST and PSI-BLAST: a new generation of protein database search programs,
627 *Nucleic acids research*, 25 (1997) 3389-3402.
- 628 [32] H.M. Berman, J. Westbrook, Z. Feng, G. Gilliland, T.N. Bhat, H. Weissig, I.N.
629 Shindyalov, P.E. Bourne, The protein data bank, *Nucleic Acids Research*, 28 (2000) 235-242.
- 630 [33] P. Emsley, B. Lohkamp, W.G. Scott, K. Cowtan, Features and development of Coot,
631 *Acta Crystallographica Section D: Biological Crystallography*, 66 (2010) 486-501.
- 632 [34] W.F. van Gunsteren, S. Billeter, A. Eising, P. Hünenberger, P. Krüger, A. Mark, W.
633 Scott, I. Tironi, *Biomolecular simulation: the GROMOS96 manual and user guide*, Vdf
634 Hochschulverlag AG an der ETH Zürich, Zürich, 86 (1996) 1-1044.
- 635 [35] S. Dallakyan, A.J. Olson, *Small-molecule library screening by docking with PyRx*,
636 *Chemical biology*, Springer, Place Published, 2015, pp. 243-250.
- 637 [36] O. Trott, A.J. Olson, AutoDock Vina: improving the speed and accuracy of docking with
638 a new scoring function, efficient optimization, and multithreading, *Journal of computational*
639 *chemistry* 31 (2010) 455-461.
- 640 [37] A. Pomerantsev, K. Kalnin, M. Osorio, S. Leppla, Phosphatidylcholine-specific
641 phospholipase C and sphingomyelinase activities in bacteria of the *Bacillus cereus* group,
642 *Infection and Immunity*, 71 (2003) 6591-6606.
- 643 [38] A. Takeno, A. Okamoto, K. Tori, K. Oshima, H. Hirakawa, H. Toh, N. Agata, K.
644 Yamada, N. Ogasawara, T. Hayashi, Complete genome sequence of *Bacillus cereus* NC7401,
645 which produces high levels of the emetic toxin cereulide, *Am Soc Microbiol*, 2012.
- 646 [39] Z. Xiong, Y. Jiang, D. Qi, H. Lu, F. Yang, J. Yang, L. Chen, L. Sun, X. Xu, Y. Xue,
647 Complete genome sequence of the extremophilic *Bacillus cereus* strain Q1 with industrial
648 applications, *Journal of Bacteriology*, 191 (2009) 1120-1121.
- 649 [40] S.F. Martin, M.R. Spaller, P.J. Hergenrother, Expression and site-directed mutagenesis of
650 the phosphatidylcholine-preferring phospholipase C of *Bacillus cereus*: probing the role of the
651 active site Glu146, *Biochemistry*, 35 (1996) 12970-12977.
- 652 [41] C.A. Tan, M.J. Hehir, M.F. Roberts, Cloning, Overexpression, Refolding, and
653 Purification of the Nonspecific Phospholipase C from *Bacillus cereus*, *Protein Expression and*
654 *Purification*, 10 (1997) 365-372.

- 655 [42] S. Kurioka, M. Matsuda, Phospholipase C assay using p-nitrophenylphosphorylcholine
656 together with sorbitol and its application to studying the metal and detergent requirement of
657 the enzyme, *Analytical Biochemistry*, 75 (1976) 281-289.
- 658 [43] M. El-Sayed, M. Roberts, Charged detergents enhance the activity of phospholipase C
659 (*Bacillus cereus*) towards micellar short-chain phosphatidylcholine, *Biochimica et Biophysica*
660 *Acta (BBA)-Protein Structure and Molecular Enzymology*, 831 (1985) 133-141.
- 661 [44] V.G. Eijsink, S. Gåseidnes, T.V. Borchert, B. Van Den Burg, Directed evolution of
662 enzyme stability, *Biomolecular Engineering*, 22 (2005) 21-30.
- 663 [45] B. van den Burg, V.G. Eijsink, Selection of mutations for increased protein stability,
664 *Current Opinion in Biotechnology* 13 (2002) 333-337.
- 665 [46] S.F. Martin, B.C. Follows, P.J. Hergenrother, B.K. Trotter, The choline binding site of
666 phospholipase C (*Bacillus cereus*): insights into substrate specificity, *Biochemistry*, 39 (2000)
667 3410-3415.
- 668 [47] Q. He, J. Li, Dynamic and morphological investigation of phospholipid monolayer
669 hydrolysis by phospholipase C, *Biochemical and Biophysical Research Communications*, 300
670 (2003) 541-545.
- 671 [48] S.R. James, A. Paterson, T.K. Harden, R.A. Demel, C.P. Downes, Dependence of the
672 activity of phospholipase C β on surface pressure and surface composition in phospholipid
673 monolayers and its implications for their regulation, *Biochemistry*, 36 (1997) 848-855.
- 674 [49] Q. He, J. Li, Hydrolysis characterization of phospholipid monolayers catalyzed by
675 different phospholipases at the air-water interface, *Advances in Colloid and Interface*
676 *Science*, 131 (2007) 91-98.
- 677 [50] G. Basáñez, J.-L. Nieva, F.M. Goñi, A. Alonso, Origin of the lag period in the
678 phospholipase C cleavage of phospholipids in membranes. Concomitant vesicle aggregation
679 and enzyme activation, *Biochemistry*, 35 (1996) 15183-15187.
- 680 [51] L.K. Nielsen, J. Risbo, T.H. Callisen, T. Bjørnholm, Lag-burst kinetics in phospholipase
681 A2 hydrolysis of DPPC bilayers visualized by atomic force microscopy, *Biochimica et*
682 *Biophysica Acta (BBA)-Biomembranes*, 1420 (1999) 266-271.
- 683 [52] A. Gericke, H. Hühnerfuss, IR reflection absorption spectroscopy: a versatile tool for
684 studying interfacial enzymatic processes, *Chemistry and Physics of Lipids*, 74 (1994) 205-
685 210.
- 686 [53] H. Horchani, L. Sabrina, L. Régine, A. Sayari, Y. Gargouri, R. Verger, Heterologous
687 expression and N-terminal His-tagging processes affect the catalytic properties of
688 staphylococcal lipases: a monolayer study, *Journal of Colloid and Interface Science*, 350
689 (2010) 586-594.
- 690 [54] F. Wang, H. Zhang, Z. Zhao, R. Wei, B. Yang, Y. Wang, Recombinant lipase from
691 *Gibberella zeae* exhibits broad substrate specificity: a comparative study on emulsified and
692 monomolecular substrate, *International Journal of Molecular Sciences*, 18 (2017) 1535.
- 693 [55] T. Johansen, T. Holm, P.H. Guddal, K. Sletten, F.B. Haugli, C. Little, Cloning and
694 sequencing of the gene encoding the phosphatidylcholine-preferring phospholipase C of
695 *Bacillus cereus*, *Gene*, 65 (1988) 293-304.

- 696 [56] C.G. Wang, M.K. Chen, T. Chen, Improved purification and some properties of a novel
697 phospholipase C from *Bacillus mycoides* strain 970, *African Journal of Microbiology*
698 *Research*, 4 (2010) 523-526.
- 699 [57] B.F. Szuhaj, *Lecithins: sources, manufacture & uses*, The American Oil Chemists
700 Society, Place Published, 1989.
- 701 [58] K. Sampaio, N. Zyaykina, E. Uitterhaegen, W. De Greyt, R. Verhé, A. de Almeida
702 Meirelles, C. Stevens, Enzymatic degumming of corn oil using phospholipase C from a
703 selected strain of *Pichia pastoris*, *LWT - Food Science and Technology*, 107 (2019) 145-150.
- 704 [59] G. Van Meer, D.R. Voelker, G.W. Feigenson, Membrane lipids: where they are and how
705 they behave, *Nature Reviews Molecular Cell Biology*, 9 (2008) 112-124.
- 706 [60] D. Saikia, N.K. Bordoloi, P. Chattopadhyay, S. Choklingam, S.S. Ghosh, A.K.
707 Mukherjee, Differential mode of attack on membrane phospholipids by an acidic
708 phospholipase A2 (RVVA-PLA2-I) from *Daboia russelli* venom, *Biochimica et Biophysica*
709 *Acta -Biomembranes*, 1818 (2012) 3149-3157.
- 710 [61] Z. Zarai, A.B. Bacha, H. Horchani, S. Bezzine, N. Zouari, Y. Gargouri, H. Mejdoub, A
711 novel hepatopancreatic phospholipase A2 from *Hexaplex trunculus* with digestive and toxic
712 activities, *Archives of Biochemistry and Biophysics*, 494 (2010) 121-129.
- 713 [62] H. Louati, N. Krayem, A. Fendri, I. Aissa, M. Sellami, S. Bezzine, Y. Gargouri, A
714 thermoactive secreted phospholipase A2 purified from the venom glands of *Scorpio maurus*:
715 relation between the kinetic properties and the hemolytic activity, *J Toxicon*, 72 (2013) 133-
716 142.
- 717 [63] M.S. Gilmore, A.L. Cruz-Rodz, M. Leimeister-Wächter, J. Kreft, W. Goebel, A *Bacillus*
718 *cereus* cytolytic determinant, cereolysin AB, which comprises the phospholipase C and
719 sphingomyelinase genes: nucleotide sequence and genetic linkage, *Journal of Bacteriology*,
720 171 (1989) 744-753.
- 721 [64] T. Lindbäck, P.E. Granum, *Bacillus cereus* phospholipases, enterotoxins, and other
722 hemolysins, *The Comprehensive Sourcebook of Bacterial Protein Toxins*, 4th ed. Alouf, J.,
723 Ladant, D., Popoff, MR, Eds, (2015) 839-857.
- 724 [65] J.B. N'goma, M. Schué, F. Carriere, A. Geerlof, S. Canaan, Evidence for the cytotoxic
725 effects of *Mycobacterium tuberculosis* phospholipase C towards macrophages, *Biochimica et*
726 *Biophysica Acta -Molecular and Cell Biology of Lipids* 1801 (2010) 1305-1313.
- 727 [66] B.M. Castro, M. Prieto, L.C. Silva, Ceramide: a simple sphingolipid with unique
728 biophysical properties, *Progress in Lipid Research* 54 (2014) 53-67.
- 729 [67] F.M. Goñi, A. Alonso, Structure and functional properties of diacylglycerols in
730 membranes, *Progress in Lipid Research*, 38 (1999) 1-48.
- 731 [68] B. Stancevic, R. Kolesnick, Ceramide-rich platforms in transmembrane signaling, *FEBS*
732 *Letters*, 584 (2010) 1728-1740.
- 733 [69] A. Bourtsala, D. Galanopoulou, Phospholipases, *Encyclopedia of Food Chemistry*,
734 (2019).

735 [70] A. Gründling, M.D. Gonzalez, D.E. Higgins, Requirement of the *Listeria monocytogenes*
736 broad-range phospholipase PC-PLC during infection of human epithelial cells, *Journal of*
737 *Bacteriology*, 185 (2003) 6295-6307.

738 [71] B.J. Heffernan, B. Thomason, A. Herring-Palmer, L. Shaughnessy, R. McDonald, N.
739 Fisher, G.B. Huffnagle, P. Hanna, *Bacillus anthracis* phospholipases C facilitate macrophage-
740 associated growth and contribute to virulence in a murine model of inhalation anthrax,
741 *Infection and Immunity*, 74 (2006) 3756-3764.

742 [72] L.-R. Montes, F.M. Goñi, N.C. Johnston, H. Goldfine, A. Alonso, Membrane fusion
743 induced by the catalytic activity of a phospholipase C/sphingomyelinase from *Listeria*
744 *monocytogenes*, *Biochemistry*, 43 (2004) 3688-3695.

745

746

747 **Figure captions**

748 **Figure 1:** Principle of the coupled assay for determining PC-PLC_{Bt} activity using
749 phospholipid monolayers as substrates. rSmL was injected first into the subphase at a fixed
750 final amount of 40 ng and nPC-PLC_{Bt} or rPC-PLC_{Bt} was added 10 min later. The kinetic
751 experiments were recorded as described in Material and methods.

752 **Figure 2:** Purification of the rPC-PLC_{Bt} **(A)** Chromatography of rPC-PLC_{Bt} on a Ni-NTA
753 affinity column (5 cm × 1.5 cm). The column was equilibrated with buffer A (25 mM
754 Tris-HCl buffer at pH 8.5 supplemented with 25 mM NaCl and 2 mM benzamidine).
755 Unbound proteins were washed out with the same buffer A and the rPC-PLC_{Bt} was eluted
756 with a linear gradient of imidazole from 0 to 0.2 M. The flow rate was set at 60 mL/h with a
757 fraction size of 1 mL. **(B)** Chromatography profile of rPC-PLC_{Bt} from Sephadex G-75
758 column. The column (2.5 cm × 150 cm) was equilibrated with buffer A and the rPC-PLC_{Bt}
759 elution was performed with the same buffer at a rate of 12 mL/h and 3 mL fractions were
760 collected. The rPC-PLC_{Bt} activity was measured as described in Materials and Methods using
761 egg PC as the substrate. Insert, SDS-PAGE (15% of acrylamide) analysis of rPC-PLC_{Bt} at
762 final purification step (Sephadex G-75 column). The gel was stained with Coomassie blue to
763 reveal the proteins. **Lane 1:** molecular mass marker, **lane 2:** Purified enzyme fraction eluted
764 from G-75 column.

765 **Figure 3:** **(A)** Effect of metal ions on rPC-PLC_{Bt} activity. Enzyme activity was measured at
766 increasing concentrations of Ca²⁺, Mg²⁺, and Zn²⁺ using PC as a substrate under optimal
767 conditions. The star indicates that the rPC-PLC_{Bt} measured in the absence of ions and the
768 presence of 10 mM EDTA. **(B)** Effect of increasing concentration of bile salt (NaDOC) on
769 rPC-PLC_{Bt} activity using the PC as the substrate.

770 Temperature and pH effects on rPC-PLC_{Bt} and rPC-PLC_{S188P} activity and stability.
771 Temperature **(C)** and pH **(D)** effects on enzyme activity were determined using PC as the

772 substrate under standard conditions. The thermo-stability profile (**E**) was determined by
773 incubation of the pure enzyme at different temperatures (30°C–65°C) for 1 h, and the residual
774 enzyme activity was measured under optimal conditions. The pH stability (**F**) was analyzed
775 after incubating the pure rPC-PLC_{Bt} at various pH values (from 3 to 12) for 1 h and the
776 residual activity was determined under optimal conditions.

777 **Figure 4:** Molecular modeling, docking experiment and MM/PBSA simulations. (**A**) Ribbon
778 representation of PC-PLC_{Bt} molecular model. P188 and P218 are depicted as sticks (**B**)
779 Docking of a 1,2-diacyl-*sn*-phosphoglycerol (PG) into the PC-PLC_{Bt} model. The enzyme
780 backbone is depicted as a ribbon covered by a semitransparent Van der Walls surface, while
781 PG is depicted as sticks and zinc ion as a grey sphere. The hatched arrows materialize the
782 potential motions of the protein domains. (**C**) Docking of a 1,2-diacyl-*sn*-phosphocholine
783 (PC) and of a 1,2-diacyl-*sn*-phosphoglycerol (PG) into the PC-PLC_{Bc} x-ray-structure or into
784 the PC-PLC_{Bt} model. The enzymes are covered by a Van der Walls surface, while ligands are
785 depicted as sticks. Residues that show hot-spot interactions with PC during the simulations
786 are colored in blue while ones interacting with PG are in orange (**D**) MM/PBSA binding free
787 energy calculations for PC-PLC_{Bc} and PC-PLC_{Bt} with PC or PG ligands.

788 **Figure 5:** Variation with a surface pressure of nPC-PLC_{Bt} and rPC-PLC_{Bt} on various
789 phospholipids; DLPC (**A**), DLPE (**B**), PG (**C**), and PS (**D**). PLC activity is expressed as the
790 number of moles of substrates hydrolyzed by unit time and the unit surface of the reaction
791 compartment of the “zero-order” trough.

792 **Figure 6:** rPC-PLC_{Bt} hemolytic and cytotoxic potential (**A**) Hemolytic activity of rPC-PLC_{Bt}:
793 Freshly prepared human erythrocytes were incubated with various enzyme concentrations of
794 rPC-PLC for 30 min at 37 °C. (**B**) Cell viability and cell toxicity of cultured cells (murine
795 primary chondrocytes, human prostatic cell lines WPMY-and PC-3) in the presence of 50,

796 100, and 200 $\mu\text{g}\cdot\text{mL}^{-1}$ of rPC-PLC_{Bt} .Values are expressed as mean +SD for three different
797 experiences realized in triplicate for in each group).

798

799 **List of symbols and abbreviations**

800 Bt : *Bacillus thurigiensis*

801 β -CD: β -cyclodextrin

802 DLPC: 1,2-dilauroyl-*sn*-glycero-3-phosphocholine

803 DLPE: 1,2-dilauroyl-*sn*-glycero-3-phosphoethanolamine,

804 EDTA: Ethylene diamine tetra-acetic acid

805 IPTG: Isopropyl thio-D-galactopyranoside

806 MD: Molecular dynamic

807 NaDOC: Sodium deoxycholic acid,

808 PBS: phosphate-buffered saline

809 PC-PLC: Phosphatidylcholine-specific phospholipase C

810 rPC-PLC_{Bt}: Recombinant PC-PLC of *Bacillus thurigiensis*

811 nPC-PLC_{Bt}: Native PC-PLC of *Bacillus thurigiensis*

812 PG: 1,2-diacyl-*sn*-phosphoglycerol,

813 PS: 1,2-diacyl-*sn*-phosphoserine

814 1,2-DAG: 1,2-diacylglycerol

815

Figure 1

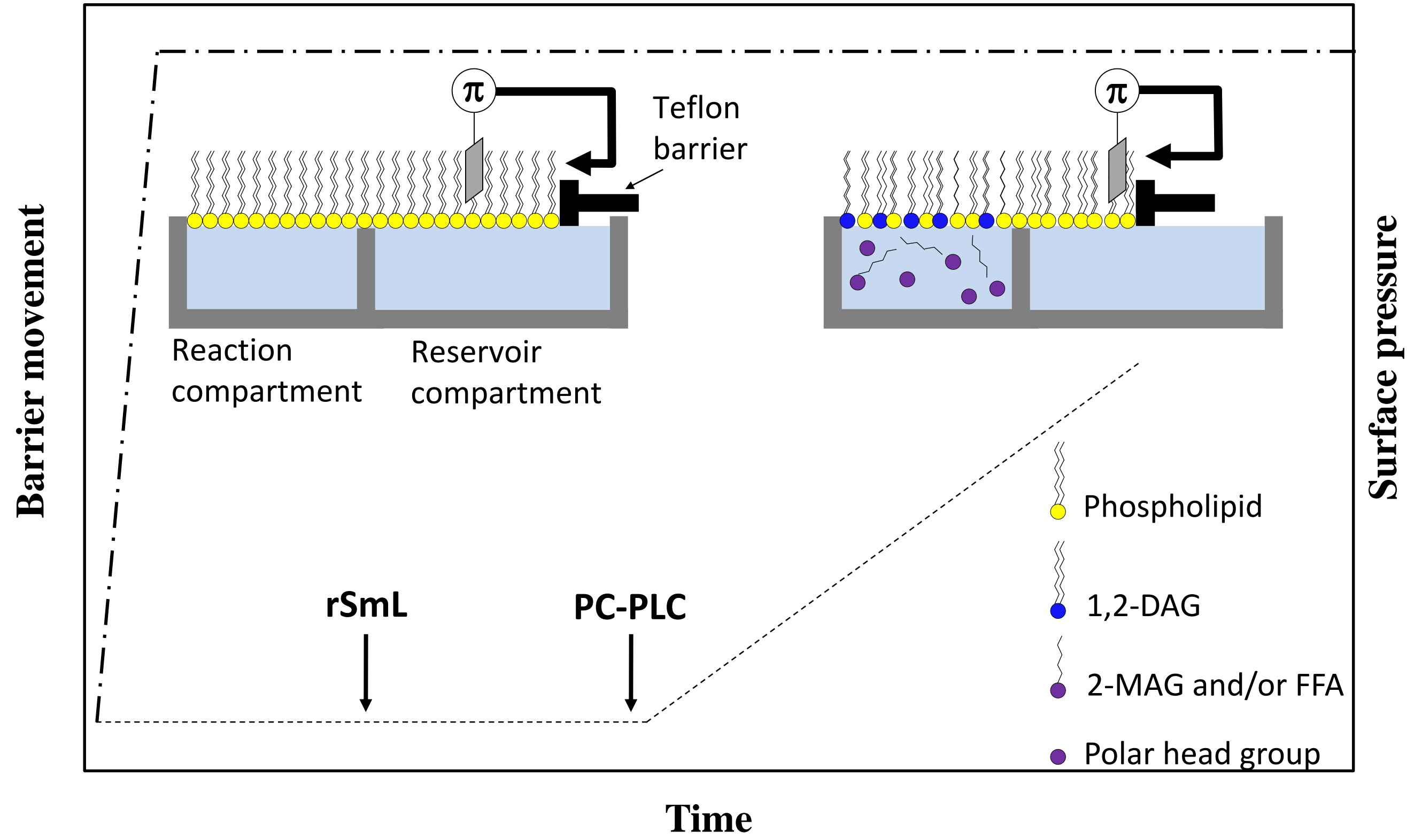


Figure 2

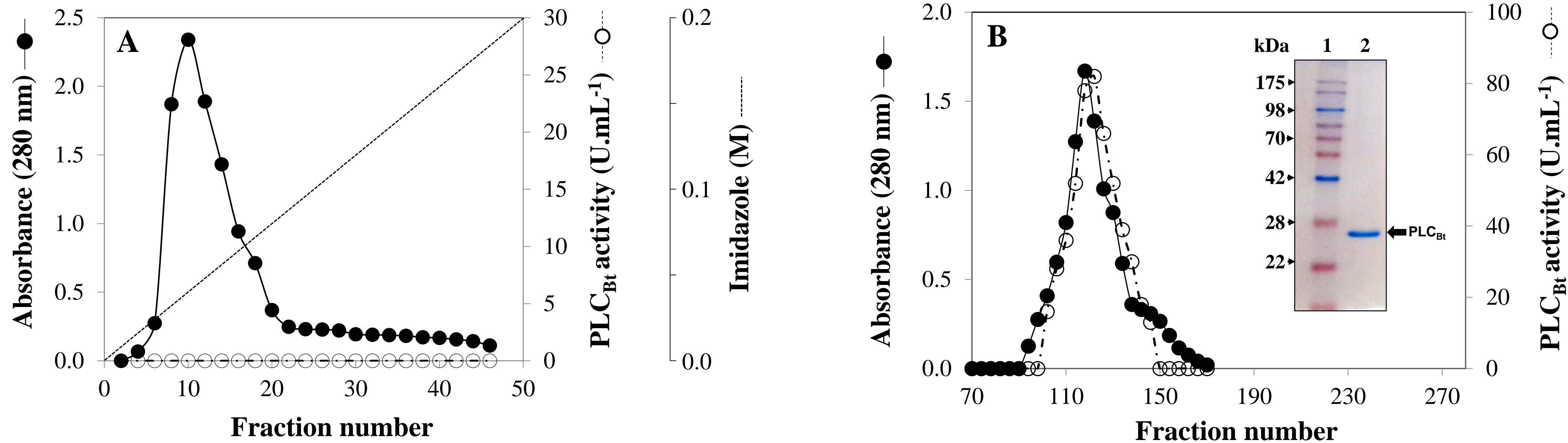


Figure 3

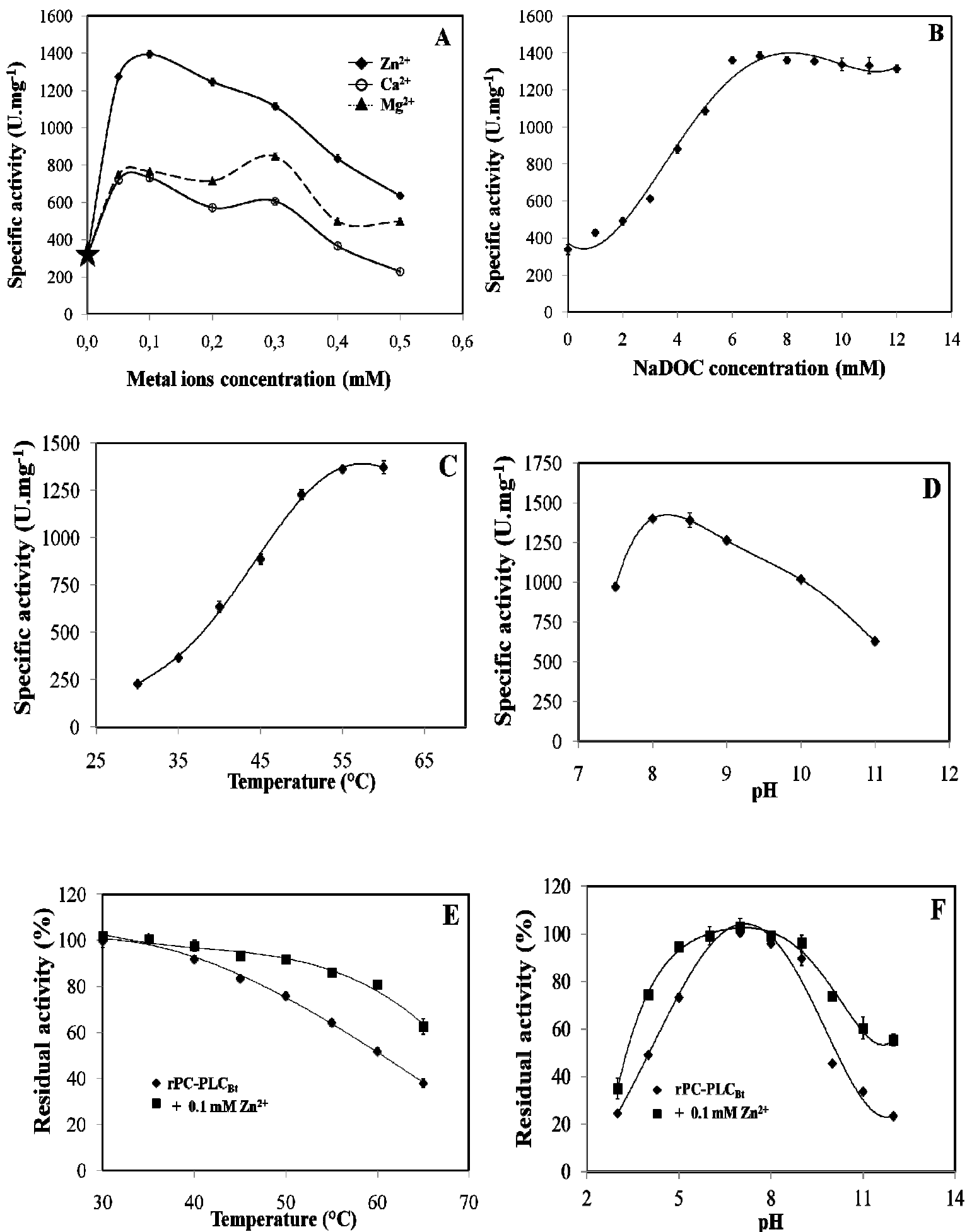


Figure 4

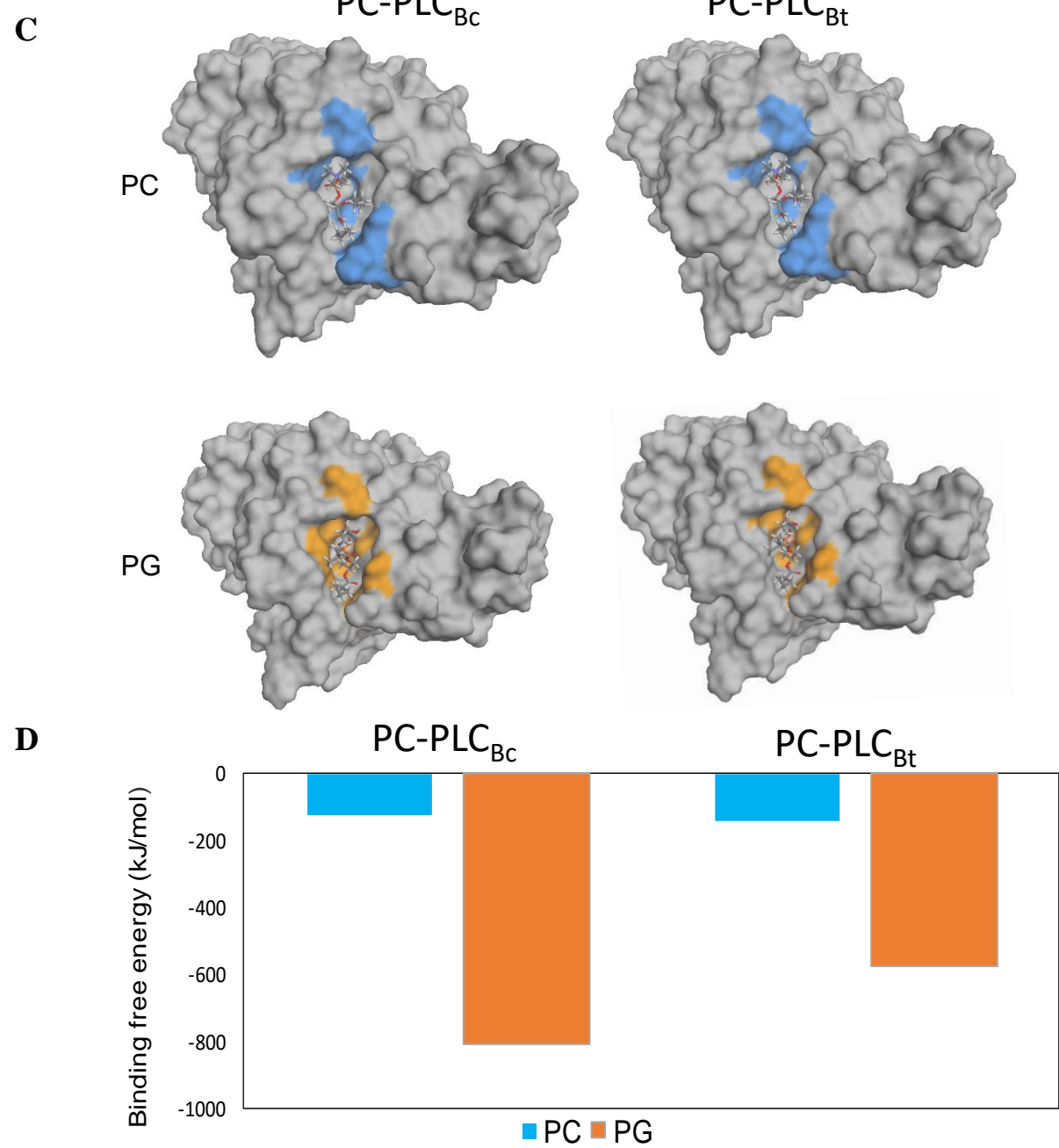
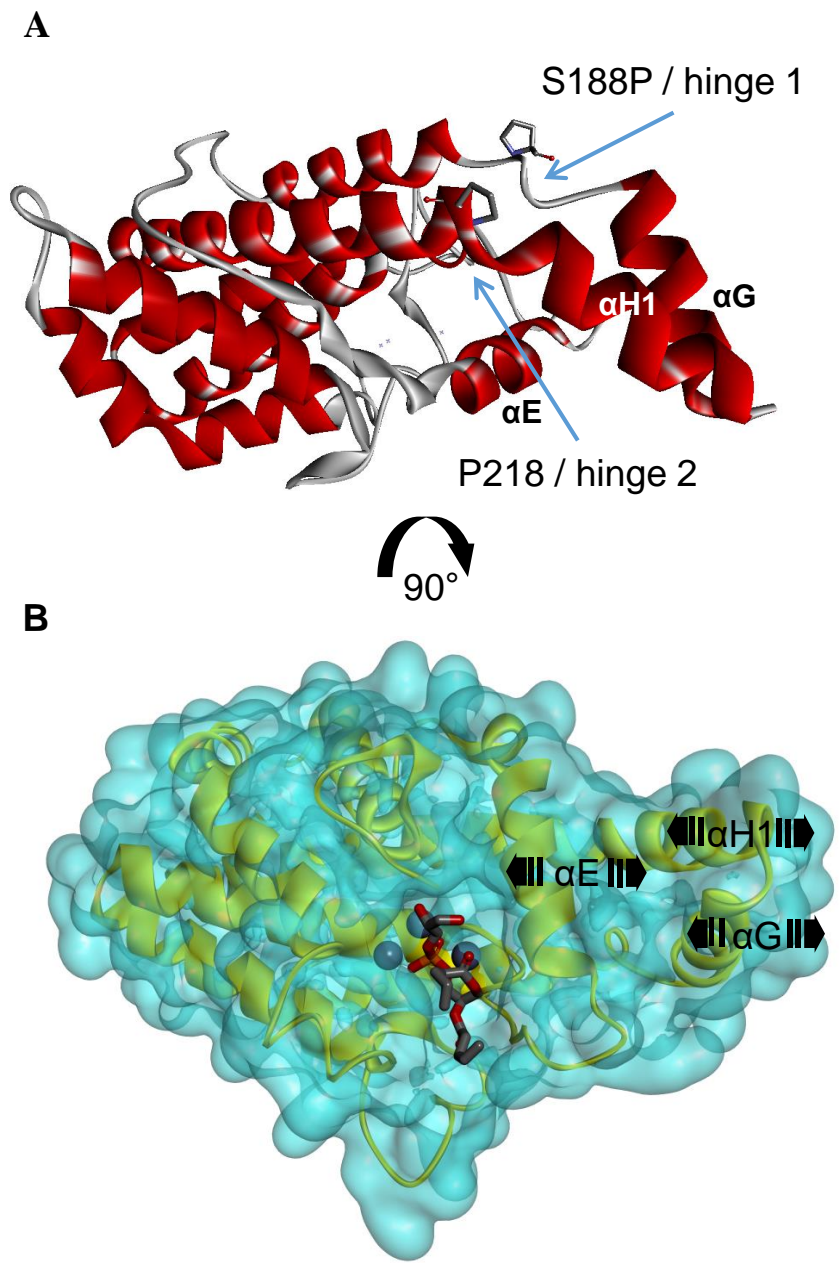


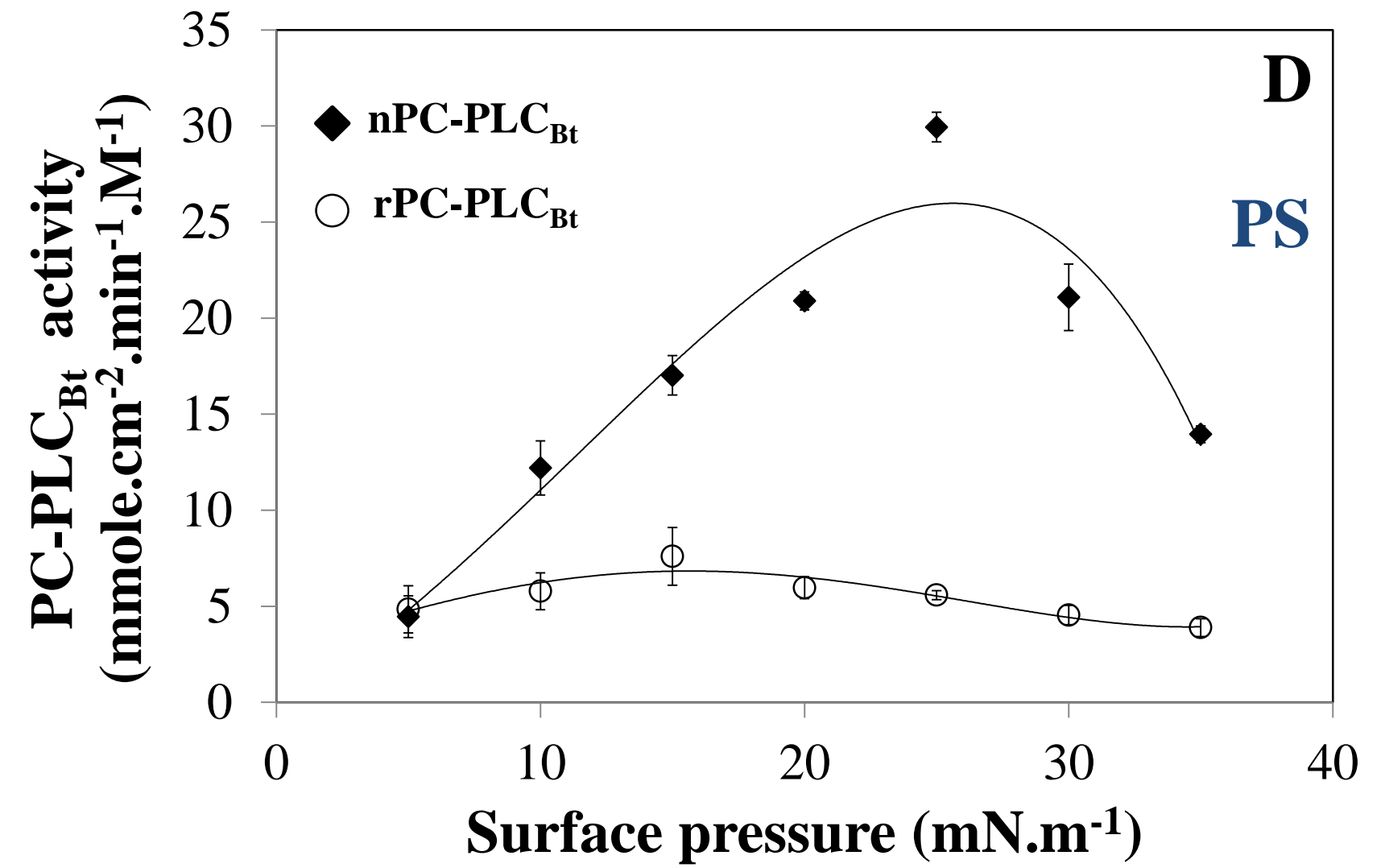
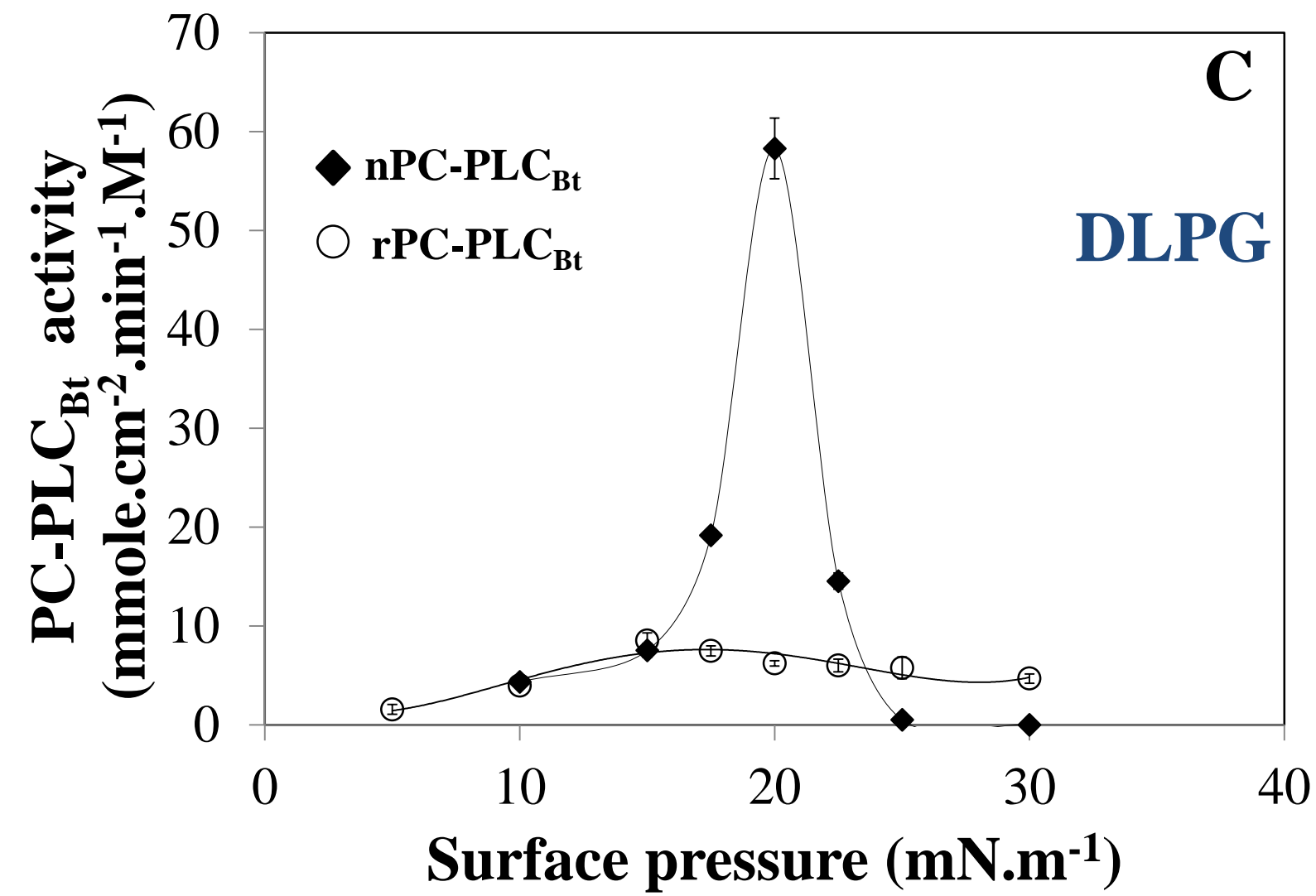
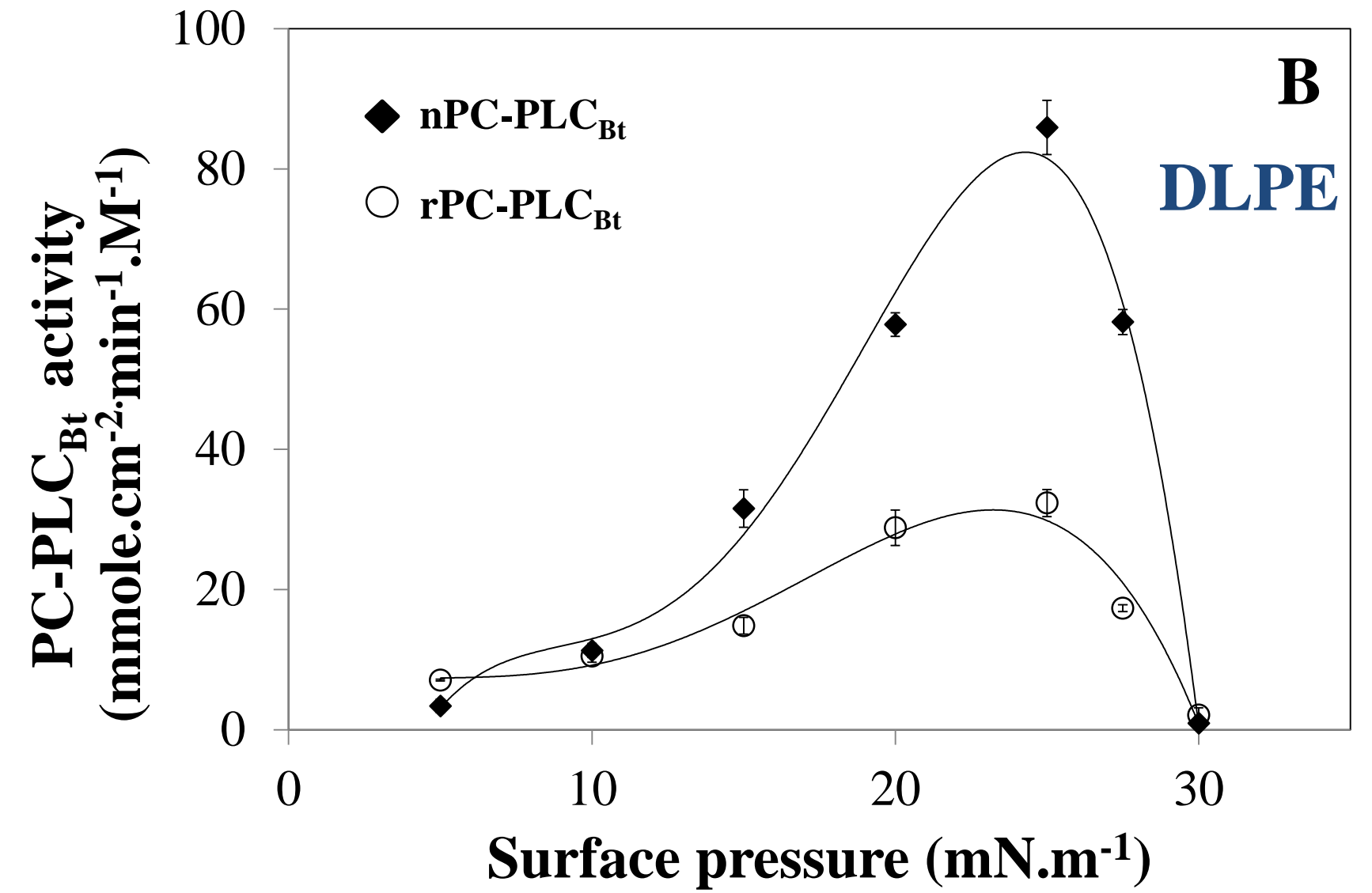
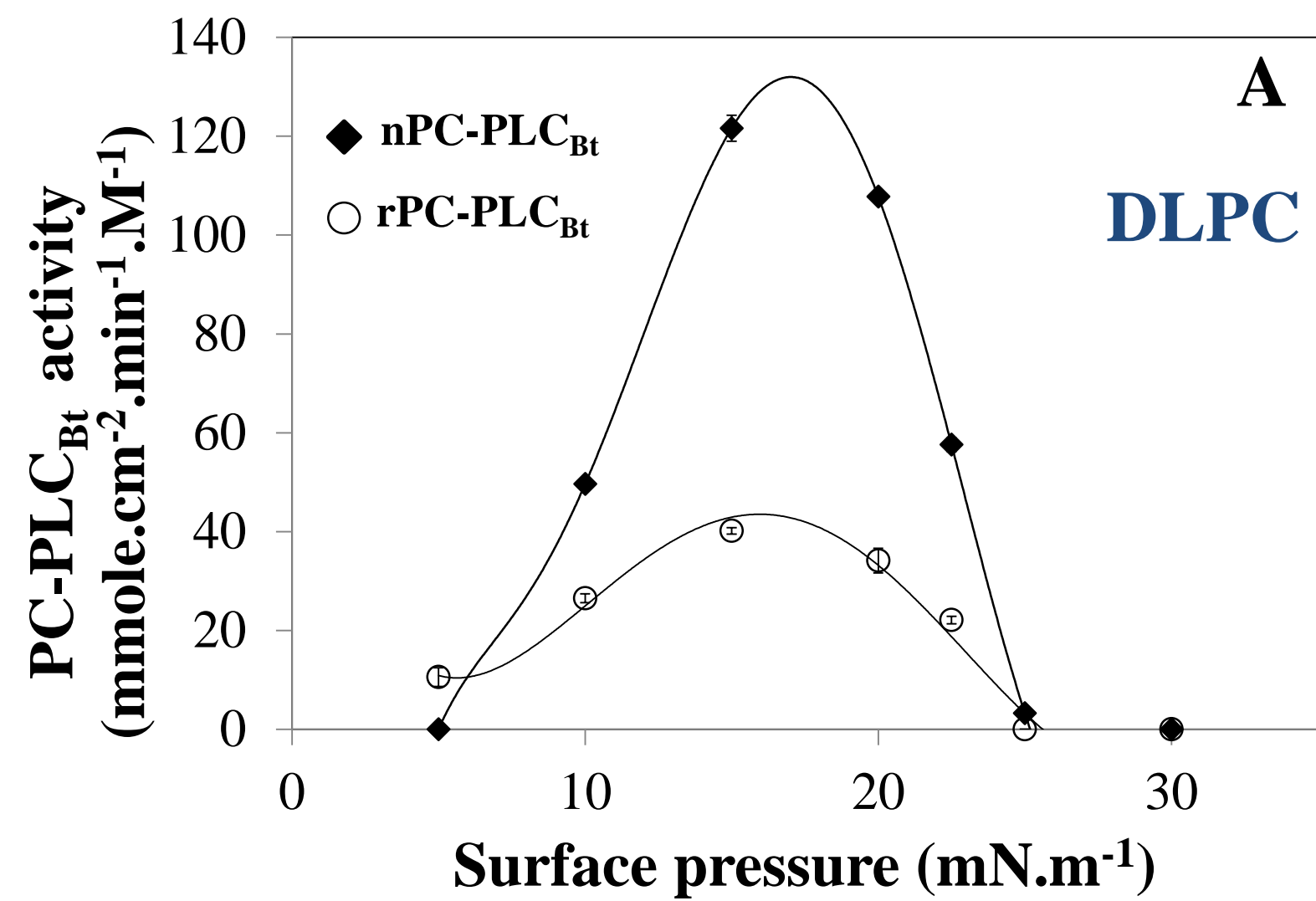
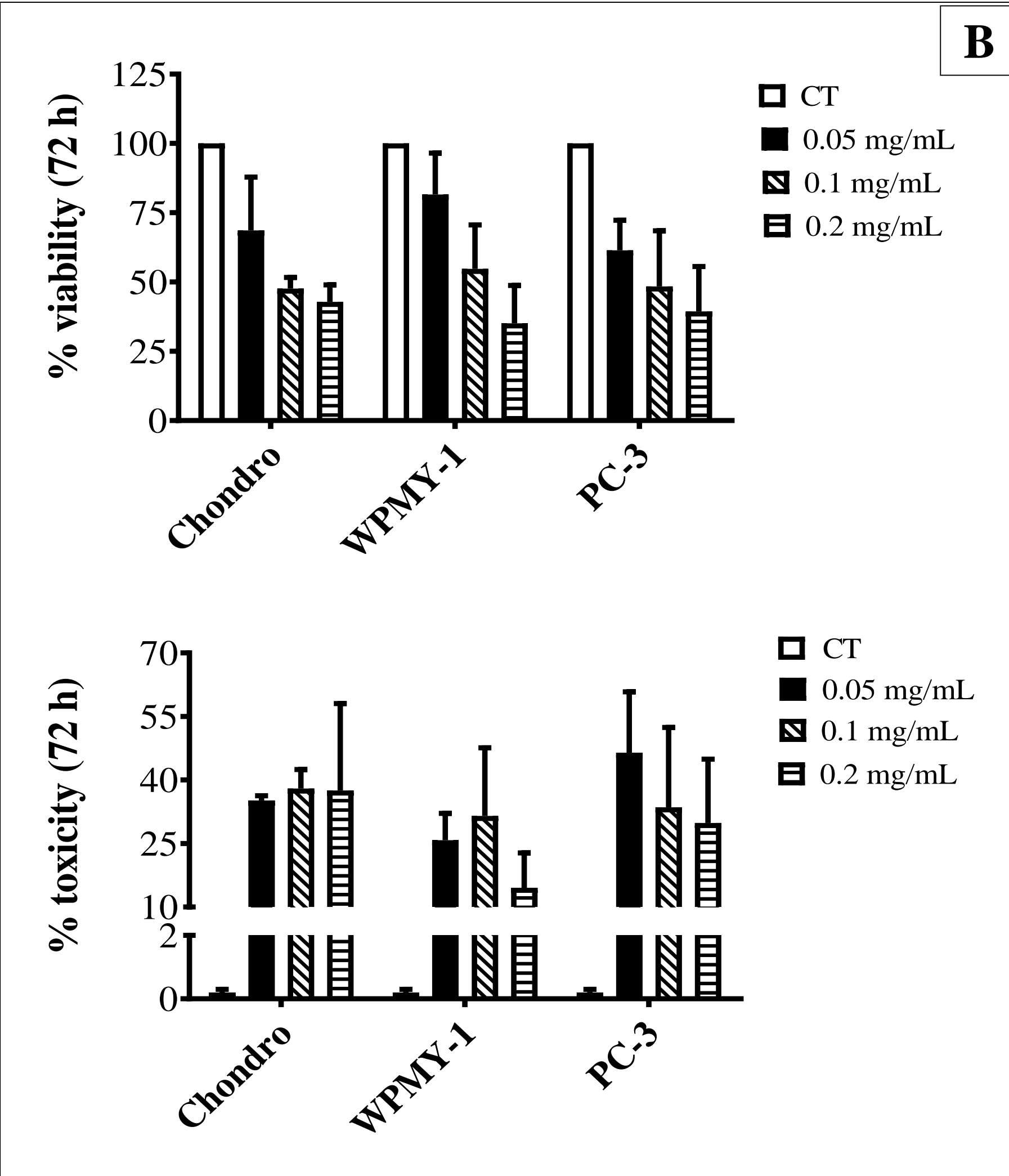
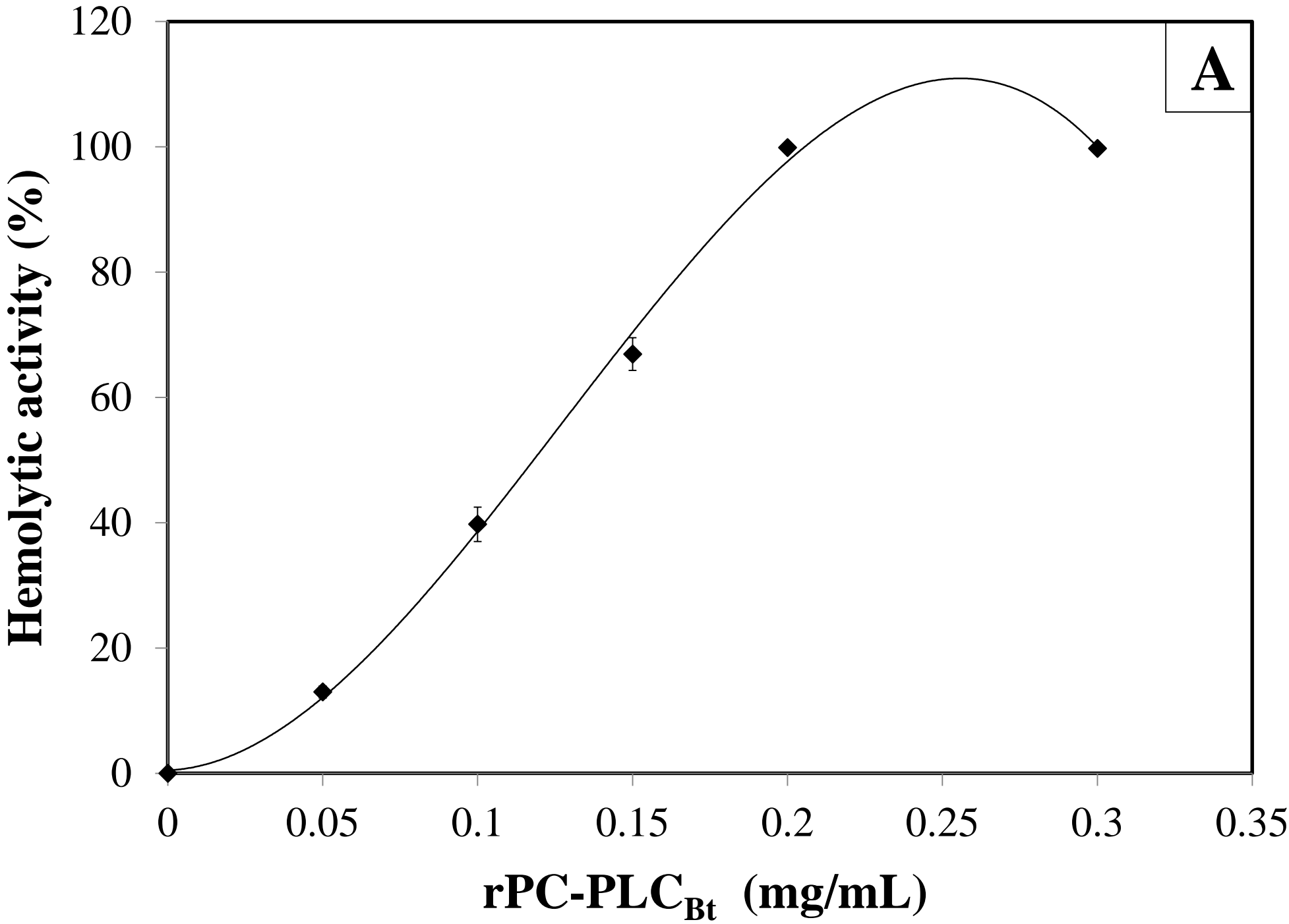
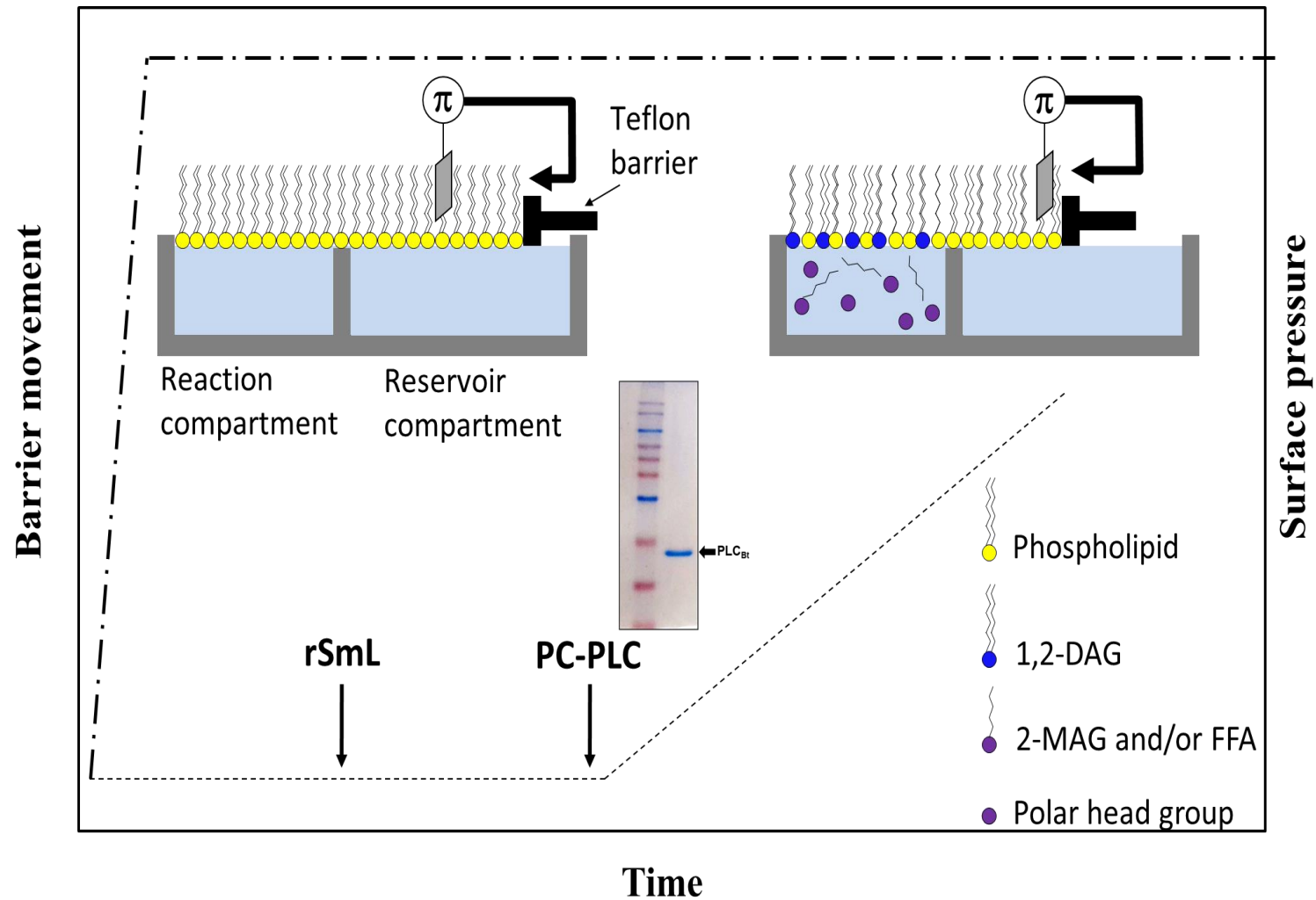
Figure 5

Figure 6

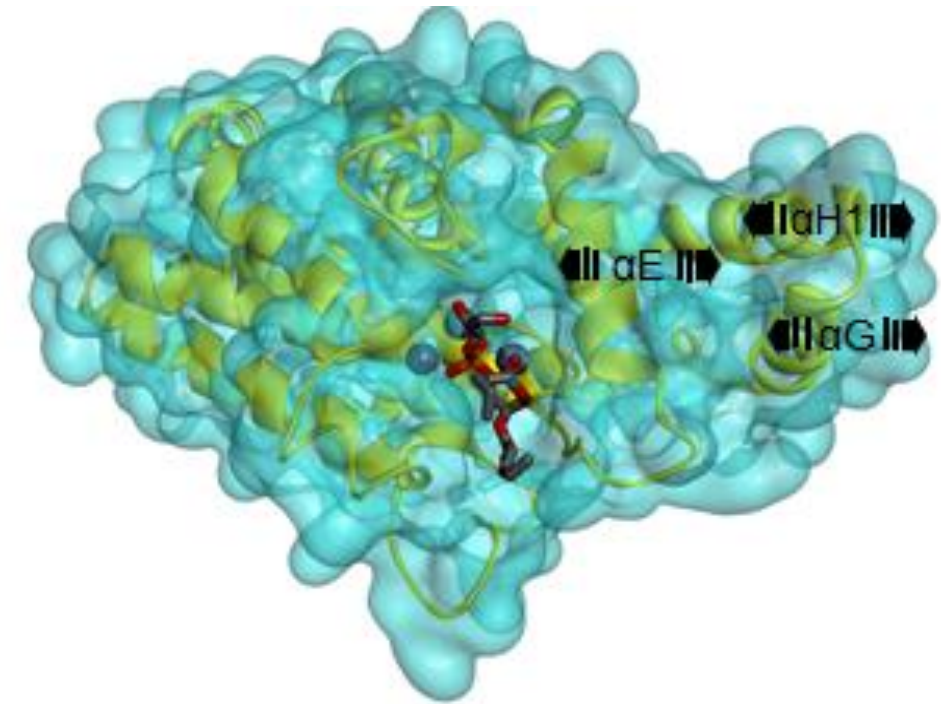


Graphical Abstract

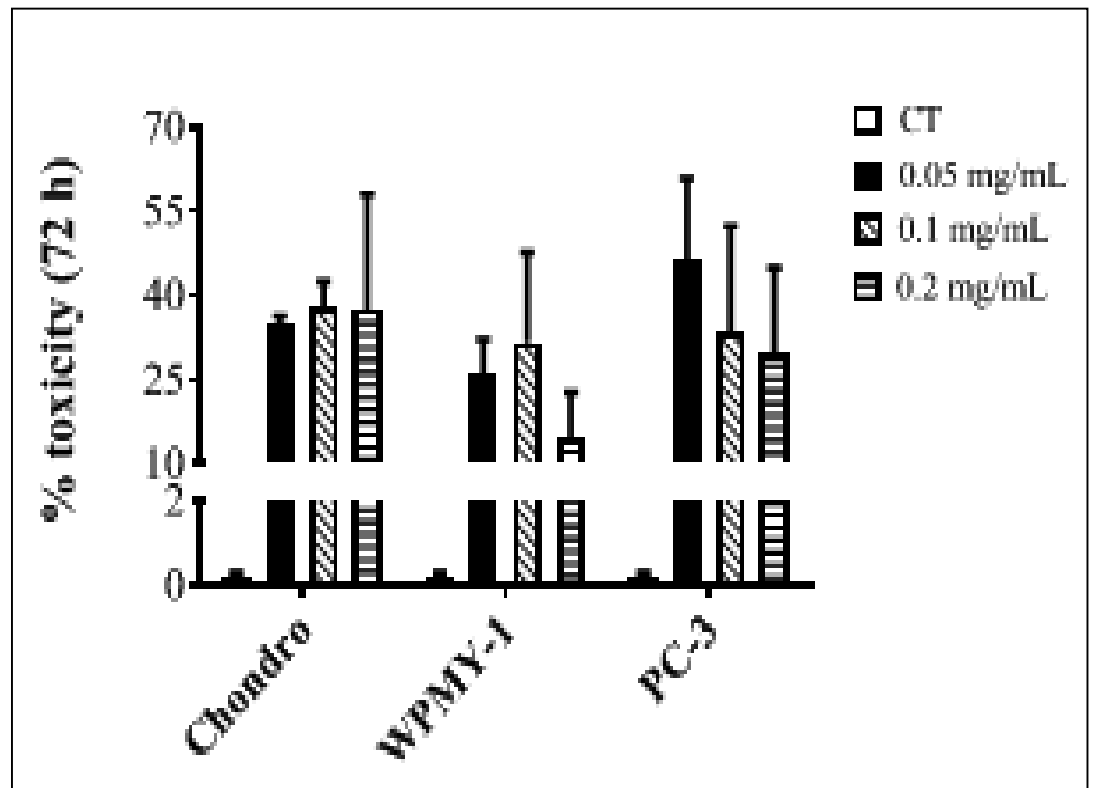
1- Expression and interfacial properties of $rPC-PLC_{Bt}$ using monomolecular film technique



2- Modeling, Molecular dynamic (MD) simulation



3- cytotoxic potential of the $rPC-PLC_{Bt}$



- ✓ *high expression yield and excellent thermophilic properties*
- ✓ *$rPC-PLC_{Bt}$ activity could be exploited for therapeutic and pharmacological purposes*
- ✓ *$PC-PLC_{Bt}$ represents a great potential in the crude oil refining industry.*